Chapter 5

Histological assessment of SJL/J mice treated with Coenzyme Q10 and Resveratrol

5.1 INTRODUCTION

The most abundant tissue in the body is represented by skeletal muscle, making up about 40% of the total body weight and is involved in many essential physiological and biochemical processes, which include heat homeostasis and metabolic integration, movement, and posture (Engel and Franzini-Armstrong, 1994; Silverthorn, 2004). The degeneration of skeletal muscle is the most common pathological feature of the muscular dystrophies (Bansal and Campbell, 2004). Muscular dystrophies characterized by dysferlin deficiency have been shown to be defective in repairing injuries to the plasma membrane (Bansal *et al*., 2003). Histopathological examinations of muscles in SJL/J mice of different ages and different sources (SJL/J, SJL/Olac) by Bittner and co-workers, disclosed features compatible with a progressive muscular dystrophy, including degenerative and regenerative changes of muscle fibers, together with a progressive fibrosis. These changes were found to primarily affect the proximal muscle groups, whereas the distal muscles remained less affected (Bittner *et al*., 1999).

Muscle morphology

Skeletal muscle is a highly specialized tissue with primary function being the generation of physical force. It is therefore more susceptible to plasma membrane damage and requires more efficient membrane repair machinery than perhaps any other tissue (Bansal and Campbell, 2004). The smallest independent cellular units of mature skeletal muscle are called fibers, also referred to as muscle cells (Kelly *et al*., 1984). Fibers are cylindrical, multinucleate, cellular structures which vary greatly in length. Fibers are grouped together into bundles called fasciculi. Within a given muscle the fibers conform to one of three modes of attachment (Kelly *et al*., 1984): *i*) those extending from one end of the fasciculus to the other; *ii*) those beginning at one or the other end of the fasciculus and terminating within the substance of the bundle; and *iii*) those having both ends within the muscular substance. Individual muscle fibers vary considerably in diameter from 10 to 100µm and may extend throughout the whole length of a muscle, reaching up to 35cm in length. In addition, the shortest fibers in small muscles are less than a millimetre in length (Kelly *et al*., 1984; Young *et al*., 2006). When viewed in cross section, the mature multinucleated muscle fiber reveals a polygonal shape (Ross *et al*., 2003). Although fibers of different thickness are intermingled in the same muscle, there

is more or less a typical size for each muscle, and some correlation has been found between the heaviness of the work a muscle performs and the thickness of its fibers (Kelly *et al*., 1984). The increase in size of a muscle which takes place during growth of an individual or which is brought about by exercise is due to an increase in the size of its fibers rather than an increase in their number (Kelly *et al*., 1984). The vast majority of the volume of each fiber is occupied by the massive cross-striated contractile organelles, the myofibrils (Kelly *et al*., 1984; Mader, 2001). Myofibrils are cylindrical in shape and run the length of the muscle fiber. With light microscopy it can be shown that the striations of myofibrils are formed by the placement of protein filaments within contractile units called sarcomeres (Mader, 2001).

The nuclei of a skeletal muscle fiber are located in the cytoplasm, immediately beneath the plasma membrane, known as the sarcolemma. They assume a position just inside the sarcolemma and usually vaguely align in rows or spirals, but occasional isolated central nuclei may be observed in histological normal muscle (Carpenter and Karpati, 1984). Peripheral nuclei are elongated parallel to the myofibrils, appearing in longitudinal sections as long ovals, 4 to 5µm in length and 1 to 2µm in width. Approximately 3.8% of nuclei in adult human muscle at the periphery of muscle fibers are those of satellite cells. These nuclei cannot be distinguished from the myonuclei in cryostat sections, but occasionally on resin sections, as they tend to have denser chromatin (Carpenter and Karpati, 1984). Also, they have a slightly more slender appearance, and a definite division between the nucleus and the sarcolemma can be observed at the ultrastrucutral level.

The sarcolemma represents the plasma membrane of the cell, its external lamina and the surrounding reticular lamina (Ross *et al*., 2003), now referred to as the sarcolemma and the basal lamina. The plasma membrane of muscle fibers is similar to that of other cells in the body in being a fluid mosaic sheath, composed of a lipid bilayer with embedded proteins (Carpenter and Karpati, 1984). The basal lamina or basement membrane of muscle fibers is attached to the outer leaflet of the plasma membrane and partly penetrated by the acidic glycoproteins of the cell coat (Carpenter and Karpati, 1984). The function of the basal lamina is believed to provide external mechanical support for the fiber and to facilitate muscle fiber regeneration (Carpenter and Karpati, 1984).

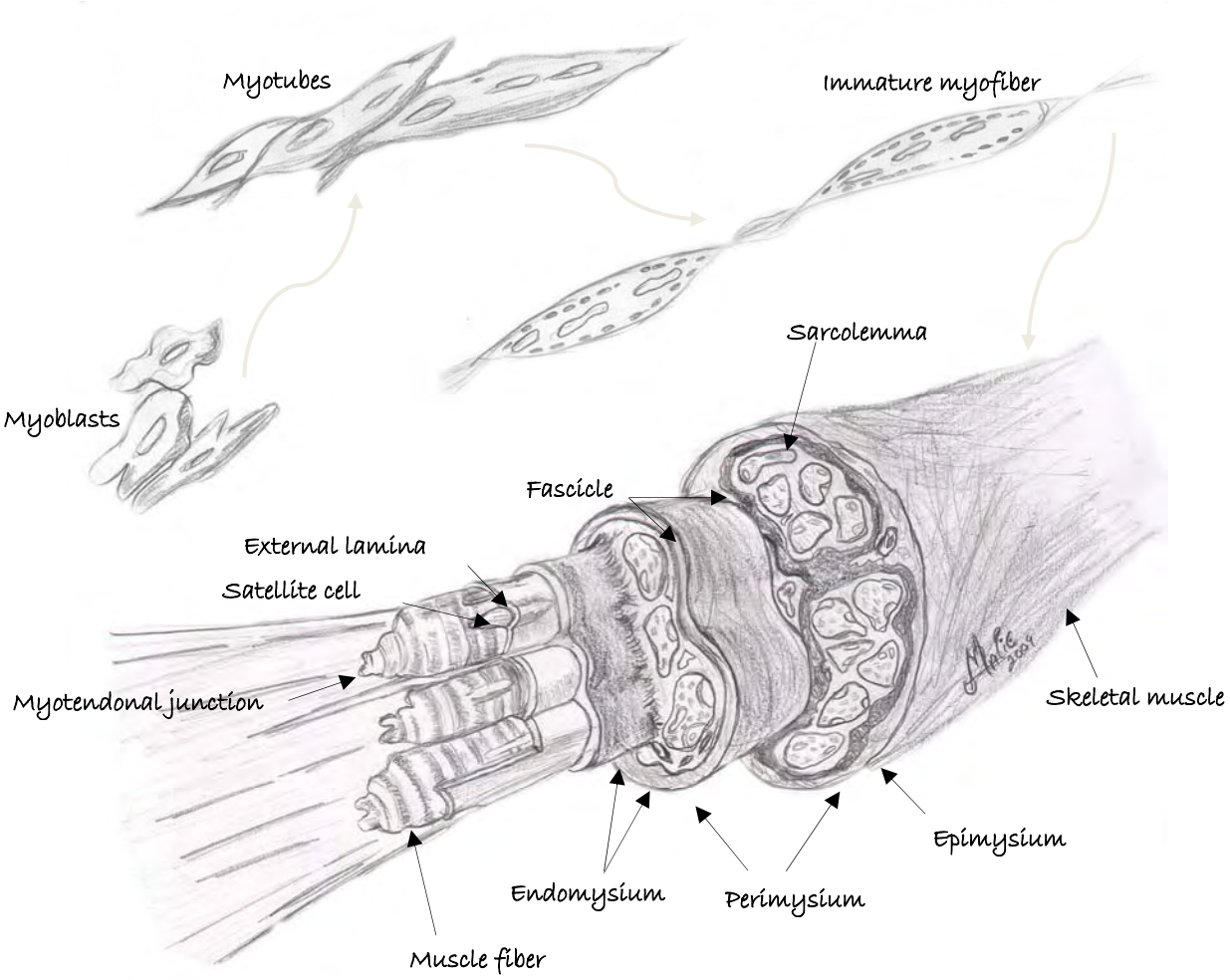

Figure 5.1: Schematic representation of skeletal muscle development and organization of muscle fibers and their connective tissue ensheathments. (Adapted from Kelly *et al*., 1984)

The connective tissue that surrounds both individual muscle fibers and bundles of muscle fibers is essential for force transduction (Ross *et al*., 2003). At the end of the muscle, the connective tissue continues as a tendon or some other arrangement of collagen fibers that attaches the muscle usually to bone. A rich supply of blood vessels and nerves travels in the connective tissue. The connective tissue associated with muscle is named according to its relationship with the muscle fibers (Figure 5.1). Endomysium is the delicate layer of reticular fibers that immediately surrounds individual muscle fibers. Only small-diameter capillaries and the finest neuronal branches are present within the endomysium, running parallel to the muscle fiber. The perimysium is a thicker connective tissue layer that surrounds a group of fibers to form a bundle or fascicle. Fascicles are functional units of muscle fibers that tend to work together to perform a specific function. Larger blood vessels and nerves travel in the perimysium. The epimysium represents the sheath of dense connective tissue

that surrounds a collection of fascicles that constitutes the muscle. The major vascular and nerve supply penetrates the epimysium (Ross *et al*., 2003).

Why histopathology assessment?

This chapter discusses skeletal muscle histopathology in the SJL/J mouse model for dysferlinopathy. Light microscopic investigation of the early pathological abnormalities in non-necrotic muscle fibers of dysferlin-deficient patients revealed that muscle specimens displayed abnormal variation of fiber size, fiber splitting, an increased number of internalized nuclei, scattered necrotic and regenerating fibers, and increased endomysial and perimysial connective tissue (Selcen *et al*., 2001). Other abnormalities consisted of small, irregularly circumscribed decreases of oxidative enzyme activity, few lobulated fibers, rare ring fibers, and sparse perivascular mononuclear cells (Selcen *et al*., 2001). Abnormal distribution of the muscle fiber size in muscle cross-section is a hallmark of the pathological changes in dystrophic muscle (Briguet *et al*., 2004). To allow for reliable quantitative assessment of fiber size variation in SJL/J quadriceps muscle, it is essential to select a method for determining the muscle fiber cross-sectional size which is not, or as little as possible influenced by the sectioning procedure. It was therefore decided to determine the variability of muscle fiber size in the SJL/J mouse model for dysferlinopathy in the current study with the minimal Feret's diameter parameter to allow for quantitative assessment of the influence of the dystrophic process on fiber size. The evaluation is based on 1µm thick resin sections since they offer by far the best morphological detail. They offer a view analogous to very-low-power electron microscopy with the advantage of a much larger sampling area (Carpenter, 2001 a), ideal for studying alterations at the cellular level.

The study of the form of structures seen with a microscope, with specific focus on the anomalies thereof, defines the purpose of the present chapter. Dysferlin deficient muscular dystrophy manifests as the result of, amongst others, a defective membrane repair mechanism. The cellular alterations, as observed with a light microscope, associated with this defect and the effect of antioxidant supplementation, are investigated. The effect of CoQ10 on cells and tissues has been proposed to be wide-ranging with the capacity to modulate diverse tissue activities and disease processes via small intrinsic cell metabolic perturbations (Linnane *et al*., 2002). In the present study the distribution of skeletal muscle lesions and the severity thereof were examined by histopathological examinations and morphometric comparison of the fiber diameter. The differences were compared between 14 and 27 week-old untreated SJL/J mice, the different 27 week-old antioxidant supplemented groups, and the 27 week-old SWR/J group, as the negative control.

5.2 Materials and Methods

5.2.1 Morphology

Quadriceps and gastrocnemius muscle samples were collected for histological investigation at termination. A small piece (± 2 x 3 mm) of muscle tissue was dissected from the belly area of the quadriceps and gastrocnemius muscles. Tissue samples were immediately fixed in 2.5% formaldehyde in 0.075 M phosphate buffer, pH 7.4 at room temperature overnight. The tissue was removed from the fixative, rinsed thrice, 10 min each, in 0.075 M phosphate buffer and serially dehydrated in 30%, 50%, 70% and 90% ethanol, followed by three changes of absolute ethanol for 15 min per dehydration step. Tissue was then infiltrated with 50% LR White Resin (SPI Supplies, West Chester, PA) in absolute ethanol for one hour, followed by infiltration with 100% LR White Resin for a minimum of four hours. Thereafter, tissue was orientated in order to produce transverse tissue sections, embedded in 100% LR White Resin and labelled accordingly. Samples were polymerized for 24 hours at 60°C. Ten to 20 serial sections of between 0.5µm to 1.5µm (optimal 1µm) were cut with a Reichert-Jung Ultra Cut E ultramicrotome (Vienna, Austria). Sections were collected onto droplets of water on Menzel glaser glass slides and dried on a slide warmer. Three slides were prepared for each tissue type of each animal. All samples were numbered with a four digit numbering system that was documented with the initial animal group, number and tissue isolated. Slides were numbered accordingly. Gill's Haematoxylin (Solulab, Johannesburg, South Africa), a general nuclear stain, together with 0.2% Toluidine Blue O (Electron Microscopy Sciences, Washington, PA) in a 0.5% Na_2CO_3 (Merck) solution (pH 11) were utilized to stain the tissue sections, in order to distinguish fibers with centrally located nuclei from fibers with peripherally located nuclei, and to determine the presence of inflammatory infiltrates and fiber size. Sections were stained with Haematoxylin for 1 hour, rinsed 10 times with water and then dehydrated on a slide warmer, followed by Toluidine Blue O staining for 30 sec, rinsed 10 times with water, followed by dehydration. Preparations were mounted with Entellan (Merck). Viewing and image capturing were done with a Nikon Optiphot transmitted light microscope (Nikon Instech Co., Kanagawa, Japan), equipped with a Nikon DXM 1200F digital camera. One to three slides from each and every sample were investigated at 20x, 40x and 100x objective lens magnification. Images from each sample were captured at 40x and 100x objective lens magnification for histological analyses. The resultant images were enhanced with Adobe Photoshop 7.0. In most instances the layers of the images were flattened and the colour from each image was removed as this produced a sharper image of the fiber periphery and other tissue components of interest. The severity of skeletal muscle lesions such as degeneration/necrosis, central nuclei and atrophy, cellular infiltration, and adipose tissue infiltration were evaluated

histopathologically and scored by a modified method of Kobayashi and co-workers. In short, histological lesions were assessed and scored as, none (0, not present), minimal (±, localized lesions), mild (+, scattered lesions), and moderate (+ +, multifocal lesions) (Kobayashi *et al*., 2009). A summary of the histological lesion assessment is given in Table 5.1.

5.2.2 Morphometry

For morphometric analyses six animals per group were randomly selected and between 10 and 20 microscopic fields for each group were captured at 20x objective lens magnification. At least 500 fibers per group were assessed for their minimal Feret's diameter (Briguet *et al*., 2004), utilizing Olympus analySIS software. All the fibers containing centrally located nuclei per microscopic field assessed, regardless of the number of centrally located nuclei (ranging from one to three), were counted. Only intact fibers were assessed for centrally located nuclei count and fiber diameter measurements, as nuclei present in cells undergoing necrosis, presumably represent those of phagocytic cells. Minimal Feret's diameter, for the assessed ≈500 cells in each experimental group, is presented in Table 5.2.

5.2.3 Statistical Analyses

For each muscle type the measured cells' diameters were then statistically compared between the various experimental groups, via Kruskal-Wallis one-way ANOVA. T-tests and Mann-Whitney U tests were also used to allow for the diameters of the gastrocnemius and quadriceps to be compared to each other within each experimental group. The statistical analyses were preformed with the use of the statistical program NCSS, with a level of significance of 0.05 being utilized during all the statistical analyses conducted.

5.3 Results and Discussion

5.3.1 Histological Findings

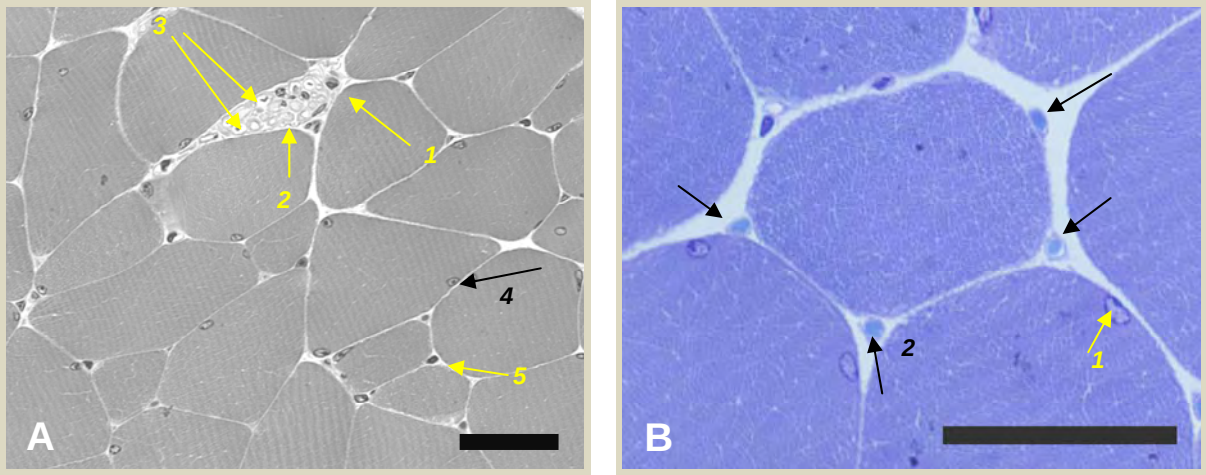

Figure 5.2: Quadriceps muscle sections from SWR/J mice at 27 weeks of age, representing the negative control group of the study. Sections were stained with Toluidine Blue O and Gill's Haematoxylin. A) A nerve bundle (1), with axons (2), and blood vessels (3) are present in this section. (B) Myonuclei (A, 4 & B, 1) and capillaries surrounding healthy myofibers (A, 5 & B, 2) are present. Scale bars = 50µm

Negative control group

Quadriceps muscle specimens analysed from all the 28 week-old SWR/J mice that represented the negative control group (Figure 5.2 A and B), displayed normal variation of fiber size. Neither inflammatory infiltrate nor active necrotic processes could be detected. Figure 5.2 A, 1 showed a nerve bundle in a transverse section. Axons (Figure 5.2 A, 2) and blood vessels (Figure 5.2 A, 3) was observed in this section. No occurrence of fiber splitting was detected while only ≈1.4% of fibers evaluated, displayed nuclei in the central position. Myonuclei (Figure 5.2 A, 4 and B, 1) were situated mostly in the peripheral position with a distribution of one to about five peripherally located nuclei per fiber. Many fibers were surrounded by a number of capillaries (Figure 5.2 A, 5 and B, 2), some displaying erythrocytes in the lumen (Figure 5.2 B, 2), while others appeared empty.

Age control group

Figures 5.3.1 and 5.3.2 display sections from the age control group, 14 week-old SJL/J mice that received no treatment. Mild (+) focal perimysial (Figure 5.3.1 A, arrow) and endomysial (Figure 5.3.1 B, arrow) inflammatory changes were observed in this group. Mononuclear cells were present between fibers (Figure 5.3.1 C, arrows). Mononuclear cells in the age control group were observed in smaller quantities, compared to that seen in the 27 week-old SJL/J groups treated with placebo.

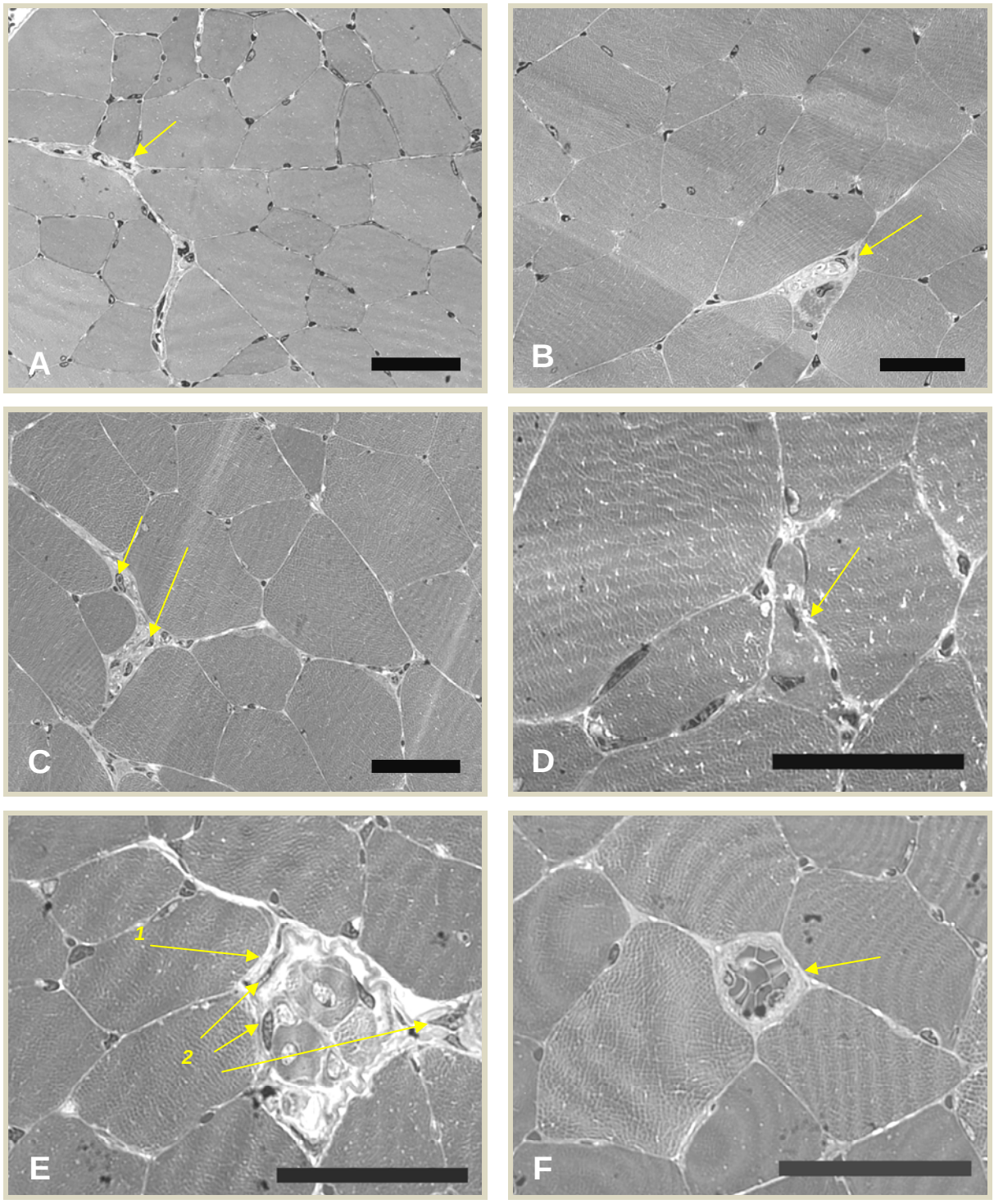

Figure 5.3.1: Quadriceps muscle sections from SJL/J mice at 14 weeks of age. Sections were stained with Toluidine Blue O and Gill's Haematoxylin. A) Perimysial and B) endomysial inflammatory changes are present (arrows). C) Mononuclear cells can be observed between fibers (arrow). D) Ongoing fiber necrosis was observed, where the degenerating fiber is invaded by mononuclear cells, presumably macrophages (arrow). E) Early stages of the necrotic process in a muscle fiber (1) with invasion by mononuclear phagocytic cells (2). F) A cluster of smooth muscle cells (arrow). Scale bars = 50µm

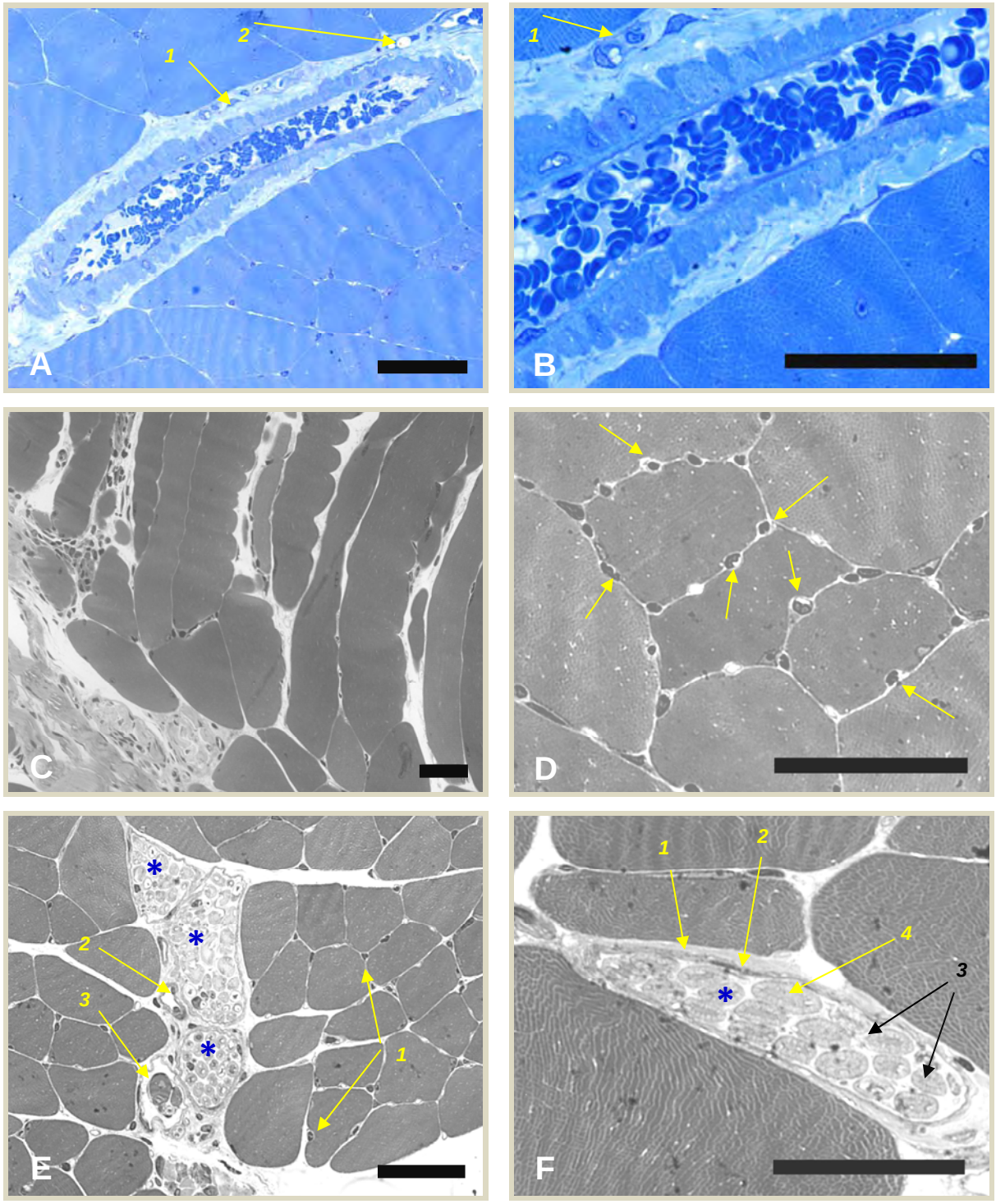

Figure 5.3.2: Quadriceps muscle sections from SJL/J mice at 14 weeks of age. Sections were stained with Toluidine Blue O and Gill's Haematoxylin. A & B) A relatively large blood vessel (arteriole) with the presence of a large number of erythrocytes in the lumen. Mononuclear cells are present in the extracellular space surrounding the arteriole (A & B, 1). Very small adipose cells are present in this region (A, 2). C) Longitudinal section of muscle fibers shows irregularly curved peripheries. D) Capillaries surrounding and indenting fibers (arrows & E, 1). E) Nerve bundles (asterisks), with blood vessels in the vicinity (2), and a muscle spindle (3) are present in the same region. F) This section display a nerve bundle with the perineurium (1), epineurium (2), individual neurons (3), and the nuclei of the perineurial cells (4) visible. Scale bars = 50µm

Necrotic fibers (Figure 5.3.1 D, arrow) were noted in regions where mononucleated cells were observed. In muscle samples from this group, mostly single fiber involvement was seen in necrotic events. These cells were often invaded by mononucleated cells presumably responsible for phagocytosis (Figure 5.3.1 D). Endomysial infiltrate (between the fibers) (Figure 5.3.1 C) was seen to a lesser extent (±) and was mostly noted around intact cells. Inflammatory infiltrate were found to be present to a lesser extent (±). 'Moth-eaten' appearance of fibers (Figure 5.3.1 D) was noted, although the overall appearance of the muscle fibers was good. Carpenter and Karpati, 1984, reported that many fibers in biopsies from limb girdle dystrophy patients show moth-eaten appearance in their centers and have prominent mitochondria along their periphery. Moth-eaten fibers have further been reported to be common in denervating conditions, though they may represent reinnervated fibers (Carpenter and Karpati, 1984).

Figure 5.3.1 E, 1, shows the early stages of an ongoing necrotic process in a muscle fiber. Invasion of the fiber by mononucleated phagocytic cells (Figure 5.3.1 E, 2) are characteristic of initial phases of the process, and these invading cells are presumably macrophages. A large number of fibers were angular in shape (Figure 5.3.1 A-F). Fiber diameter varied and ranged from 15.98 to 112.34µm, as determined by measuring the minimal Feret's diameter. Nuclei were mostly peripherally located and found in relative large numbers that vary among individuals in this group. In only 8.8% of fibers analysed, nuclei were found in the central position of the fibers.

A cluster of structures (Figure 5.3.1 F, arrow) surrounded by a multiple layered sheath was detected in one sample in this group. The smooth and shiny appearance of these structures differ markedly from the surrounding skeletal muscle fibers, and the nearest corresponding structure it could be correlated to, was smooth muscle (Carpenter and Karpati, 1984). In normal muscles smooth muscle cells are confined to the walls of veins and arteries. Carpenter and Karpati recorded a case in 1984 where there was marked independent proliferation of smooth muscle cells, accompanied by collagen in the endomysium of a limb girdle myopathy sample.

Relatively large blood vessels (Figure 5.3.2 A and B) were often observed in the age control group. Figure 5.3.2 A and B showed an arteriole, with the presence of a large number of erythrocytes in the lumen. Mononuclear cells were noted in the extracellular space surrounding the arteriole (Figure 5.3.2 A and B, 1). Very small adipose cells were also present in this region (Figure 5.3.2 A, 2). Occasional (±) fiber splitting was present in this group. On one longitudinal section, muscle fibers showed irregularly curved periphery (Figure 5.3.2 C). These indentations were of unknown cause, and remain to be further investigated at the ultrastructural level in chapter 6.

In a number of transverse sectioned samples, but not in all, numerous small circular objects were found to surround the muscle fibers (Figure 5.3.2 D, arrows, and 5.3.2, E, 1). These circular objects were compared to the work of Carpenter, 2001 a, who identified a similar occurrence as capillaries indenting a ragged-red fiber (Carpenter, 2001 a; Carpenter and Karpati, 1984). The lumens were mostly filled with erythrocytes, resulting in the dark appearance. Various nerve bundles of different sizes were observed in transverse sections from this group (Figure 5.3.2 E and F, blue asterisks). Blood vessels (Figure 5.3.2 E, 1) were often noted in these areas. A muscle spindle was identified in Figure 5.3.2 E, 3. A muscle spindle represents a specialization of certain skeletal muscle fibers and nerves to form a structure capable of giving elaborate feedback information to the nervous system on the muscle's state of activity. Muscle spindles are found relatively infrequently in routine muscle biopsies (Carpenter and Karpati, 1984). Figure 5.3.2 F, shows a larger magnification of a nerve bundle (blue asterisk). Peripheral nerves are composed of bundles of nerve fibers held together by connective tissue and a specialized layer(s) of cells, the perineurium (Figure 5.3.2 F, 1). The epineurium (Figure 5.3.2 F, 2) surrounds the bundles of nerve fibers, while the endoneurium is associated with individual neurons (Figure 5.3.2 F, 3). The nuclei of the perineurial cells (Figure 5.3.2 F, 4) appeared flat and elongated in a transverse section.

Positive control group

The quadriceps muscle specimens of 27 weeks old SJL/J mice treated with placebo (the positive control group) throughout the course of the trial, displayed abnormal variation of fiber size (Figures 5.4.1 and 5.4.2). Fiber diameter ranged between 11.82 and 99.01µm as determined by minimal Feret's diameter (Briguet *et al*., 2004). Mild (+) to moderate (+ +) perimysial inflammatory changes with endomysial involvement became predominant in this group (Figure 5.4.1). Quadriceps muscle exhibited active myopathic changes emphasized by the following findings; fiber splitting was prevalent (+) (Figure 5.4.1 A, 1 and F, 1) and its appearance was distinct in areas with more inflammatory infiltrate. Numerous necrotic fibers and fiber remnants (+ +) resultant of the ongoing necrotic processes ranging from mild (+) to moderate (+ +) were observed (Figure 5.4.1 B, 1 and D, 1). These fibers ranged from disrupted cells invaded by macrophage activity, to 'ghost' cells (Figure 5.4.1 C, 1 and E, 1), which is marked by a 'see-through' appearance of cell remnants representing the initial shape and size of the dead cell. Numerous mononucleated cells (+ +) (Figure 5.4.1 A, 2 and B, 2) were predominant in areas with inflammatory infiltrate. These cells were also found to invade fibers in the necrotic state (Figure 5.4.1 B, 3), and are presumably representative of macrophage activity.

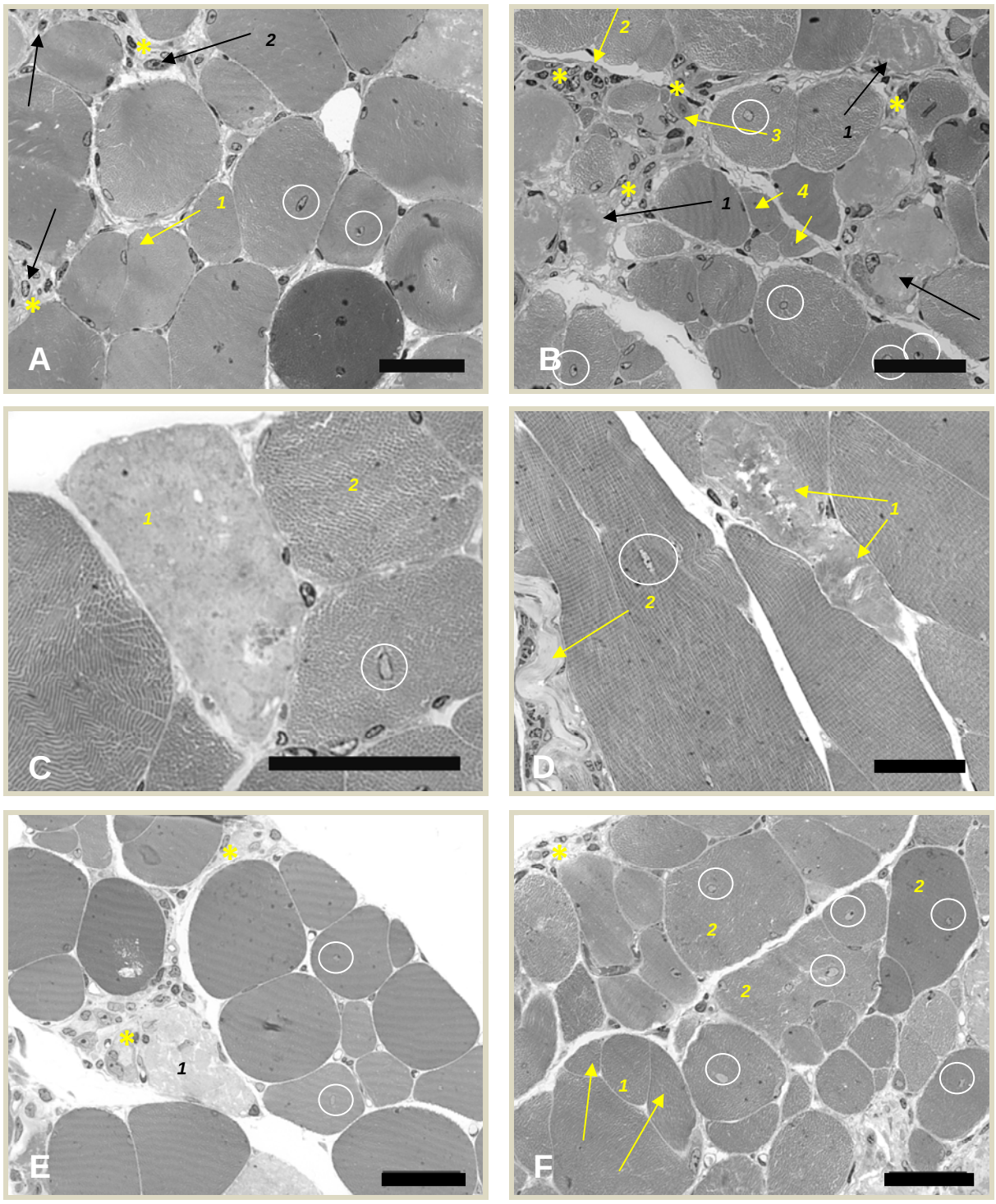

Figure 5.4.1: Quadriceps muscle sections from the positive control group; 27 week-old SJL/J mice treated with placebo. Sections were stained with Toluidine Blue O and Gill's Haematoxylin. Inflammatory infiltrate is prominent in this group (asterisks). Numerous fibers in this group display central nucleation (white circles). A) Fiber splitting is prevalent (1) and mononucleated cells are present in inflammatory regions (2). B) 'Ghost cells' (1) as a result of necrosis (asterisks) is observed. Mononucleated cells (2) are invading necrotic fibers (3). Small diameter fibers (4) are observed in nearby regions. C) Ghost cells (1) and moth-eaten appearance of cells is present. D) A necrotic fiber (1) and dense connective tissue (2) in extracellular space of fibers on a longitudinal section. E) The occurrence of ghost cells (1) in inflammatory regions (asterisk) is frequent. F) Fiber splitting (1) and hypertrophic fibers (2) are present. Scale bars = 50µm

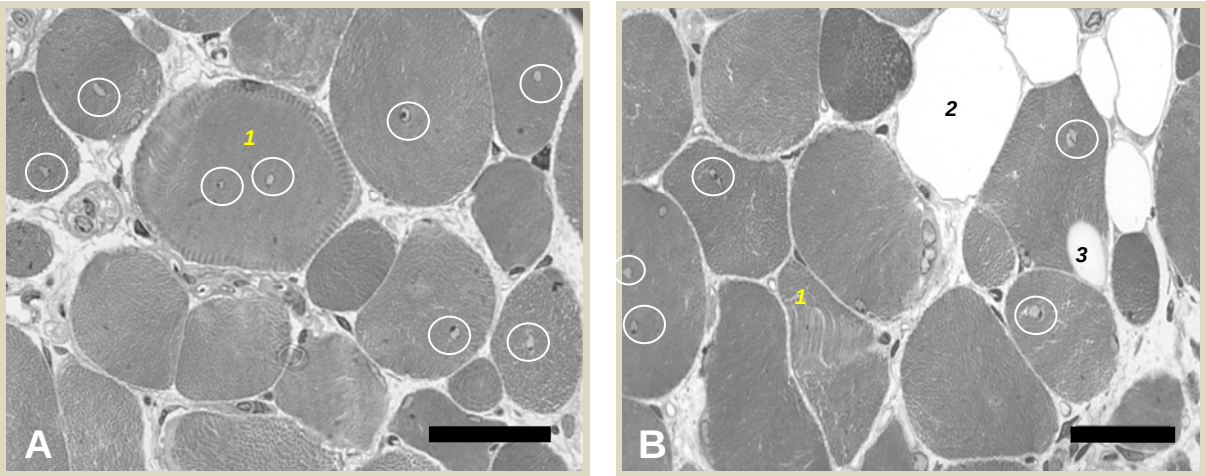

Figure 5.4.2: Quadriceps muscle sections from the positive control group; 27 week-old SJL/J mice treated with placebo (stained with Toluidine Blue O and Gill's Haematoxylin). A) Ring fibers are present (1). B) In some fibers myofibrils show a 'streaming' appearance (A, 1 & B, 1). B) Adipose cells (2) and vacuoles (3) are present. Scale bars = 50µm

The appearance of moth-eaten cells (Figure 5.4.1 C, 2) was frequent (+ +). Inflammatory infiltrate (Figure 5.4.1 A, B, E, and F, yellow asterisks) were present, ranging from mild dystrophic changes (+), characterized by numerous small diameter fibers (Figure 5.4.1 B, 4), intercepted by the occasional necrotic fibers, to moderate ongoing dystrophic processes (+ +), emphasized by large incidences of necrosis and much inflammatory infiltrate. In only one out of nine animals, no inflammatory infiltrate (0) could be detected in quadriceps muscle specimens examined, while seven out of nine showed mild (+) to moderate (+ +) dystrophic lesions and one animal showed lesions, more severe than what was classified as moderate in the present study, with up to zero intact cells in one microscopic field. This observation could possibly be explained by the possibility of inter-individual variation amongst animals, where onset of disease might have occurred later in the latter subject; or the dystrophic alterations were not affecting the muscle as a whole to the same extent. Therefore, a muscle sample showing no incidence of degeneration, might either represent an unaffected area of that specific muscle, or represent an individual likely to show full onset of the disease at a later stage.

Dense connective tissue (Figure 5.4.1 D, 2) was observed between fibers, where inflammatory infiltrate was distinctive, with a higher frequency in areas with higher necrotic incidence. Hypertrophic fibers were present and found usually together with very small fibers (Figure 5.4.1 F, 2). Ring fibers (Figure 5.4.2 A, 1) were detected in one sample from this group. Inflammatory infiltrate with mononuclear cells were present in the extracellular space surrounding this fiber. In the same sample, fibers of which the fibrils were 'streaming' (Figure 5.4.2 A and B, 2) were also seen.

In a sample from the same individual, adipose cells (Figure 5.4.2 B, 2) of which the size compared to that of the surrounding fibers, were observed. A large vacuole (Figure 5.4.2 B, 3) were noted in one of the fibers in this sample. Both angular as well as circular shaped intact fibers were present. The histological results from 6-month old, untreated, SJL/J mice were consistent with previous findings in SJL/J mice at a similar age (Weller *et al*., 1997; Ho *et al*., 2004; Suzuki *et al*., 2005; Nemoto *et al*., 2006;) and correlate with the histological findings in human dysferlinopathy patients (Gallardo *et al*., 2001; Selcen *et al*., 2001; Cenacchi *et al*., 2005).

Nuclei in the central position of fibers (white circles) were abundant and up to three central nuclei could be detected in a single fiber cross section. Nuclei in this position were found in 35.4% of fibers analysed. Peripheral nuclei were sparsely distributed along less- and unaffected fibers. The samples analysed from this group served as a baseline/reference for the experimental groups treated with the different concentrations of different antioxidants throughout the course of the trial.

Resveratrol group

A distinct variation in fiber size was apparent following qualitative histological assessment of 27 week-old SJL/J mice treated with resveratrol (60mg/kg/day). In quadriceps muscle samples analysed, minimal Feret's diameter ranged between 10.12 and 117.90µm. Angulated fibers were present although more fibers displayed a circular shape. Fiber splitting (+), was observed as groups of small nested fibers with complementary contours (Figure 5.5.1 A and B, 1). One or more of these fibers often displayed central nucleation. Mild (+) to moderate (+ +) degeneration and perimysial inflammatory changes with endomysial involvement (Figure 5.5.1 A and B, yellow asterisk) was present and underlined by the distinct presence of mononucleated cells (+) (Figure 5.5.1 A and B, 2).

The presence of necrotic fibers as 'ghost cells' (Figure 5.5.1 C, 1) as well as fiber remnants (Figure 5.5.1 A, 3), resultant of the ongoing dystrophic process was observed. Large numbers of mononucleated cells, as part of the inflammatory infiltrate were noted in areas of necrotic events. Ring fibers (Figure 5.5.1 D, 1) were detected in one sample from this group. Fibers of which the fibrils appeared to be 'streaming' (Figure 5.5.1 C, 2 and E, 1) were also seen. Mild (+) infiltration of adipose tissue ranged from very small single cell presence to colonies of more than ten adipose cells (Figure 5.5.1 E, 2) in one area of which the size compared to those of the muscle fibers. Intense vacuolation was observed in some fibers (Figure 5.5.1 F, 1). The infiltrate in perimysial spaces was mostly dense connective tissue (Figure 5.5.1 F, 2), presumably collagen. Fibroblasts (Figure 5.5.1 F, 3) with fine extending processes were found in conjunction with connective tissue infiltration.

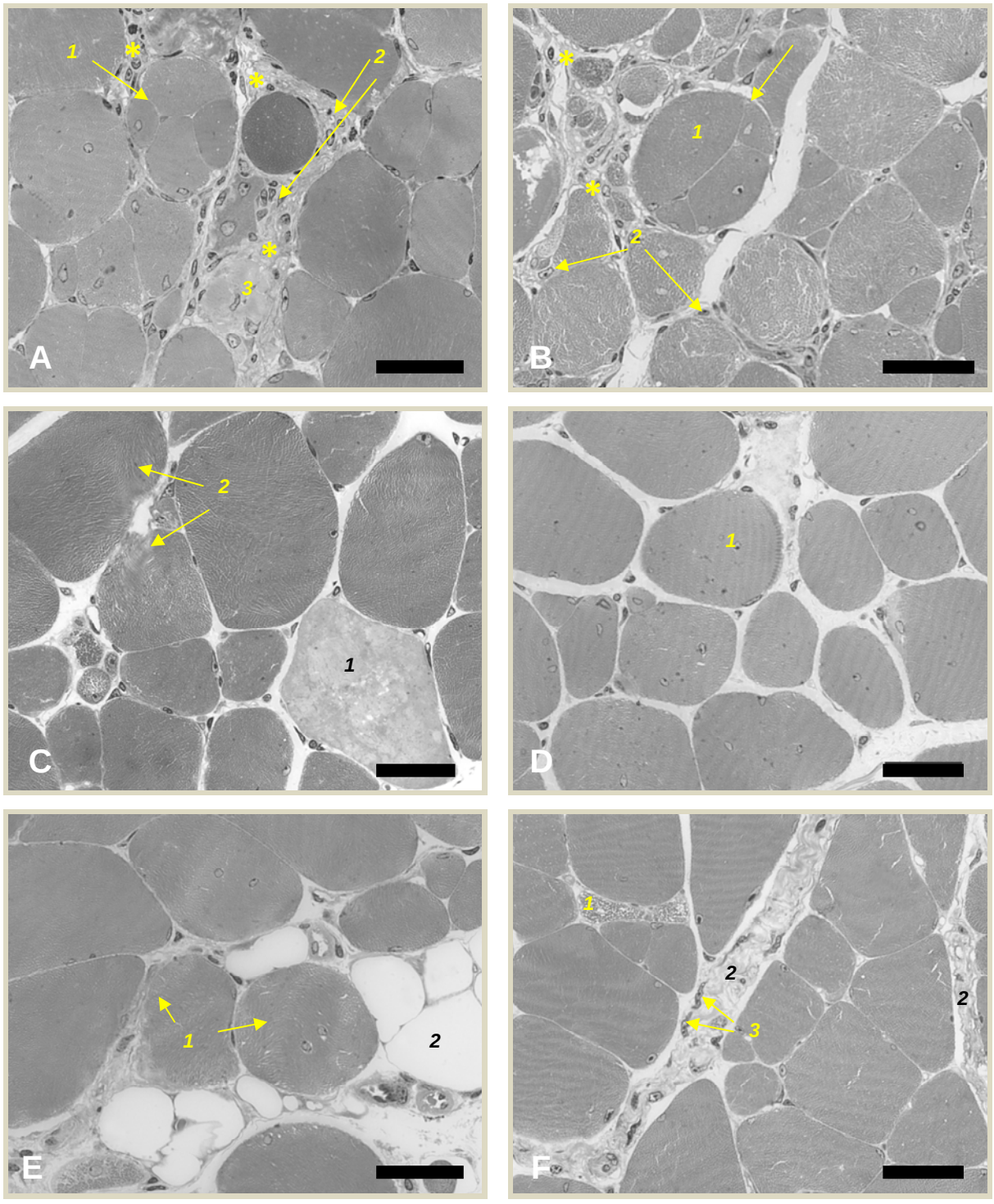

Figure 5.5.1: Quadriceps muscle sections from the 27 week-old SJL/J group treated with resveratrol. Sections were stained with Toluidine Blue O and Gill's Haematoxylin. A & B show fiber splitting as a group of nested fibers (1) in an area with moderate inflammatory infiltrate (asterisks), that contain numerous mononucleated cells (2), and fiber remnants (A, 3). C) Ghost cells (1) and fibers of which the fibrils are 'streaming' (2) can be observed. D) Ring fibers (1) are present. E) Fibers of which the myofibrils are streaming (1) in an area infiltrated by adipose cells (2). F) Vacuolation (1) occurs in fibers of this group. Connective tissue in the perimysial areas (2) are presumably collagen, with the presence of fibroblasts (3) with thin extending processes. Scale bars = 50µm

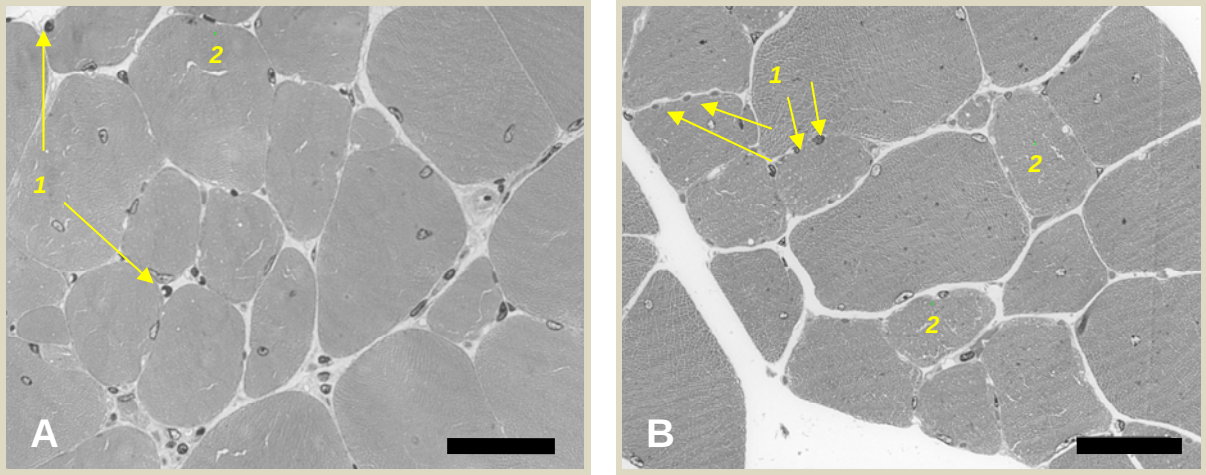

Figure 5.5.2: Quadriceps muscle sections from of the 27 week-old SJL/J group treated with resveratrol. Samples were stained with Toluidine Blue O and Gill's Haematoxylin, and display (A & B) capillaries surrounding and indenting fibers (1) and fibers which appear moth-eaten (2). Scale bars = 50µm

The presence of capillaries surrounding, and indenting fibers, (Figure 5.5.2 A and B, 1) was observed. A moderate (+ +) presence of fibers with a moth-eaten appearance (Figure 5.5.2 A and B, 2) was seen in this group. In general, fibers ranged from being intact (no incidence of dystrophic process in a specific microscopic field), healthy appearing cells with peripherally located nuclei to areas with multifocal lesions (+ +). Myonuclei in the central position of the fiber ranged from 1 to 3 nuclei per fiber with an occurrence of 31.6% in analysed quadriceps muscle samples. Evaluating from a qualitative point of view; more intact cells were detected in this group compared to the positive control group, who received only placebo.

Low CoQ10 group

A variation in fiber size was prominent, in the group of 27 week-old SJL/J mice, treated with a low concentration (40mg/kg/day) of CoQ10. Fiber diameter in this group ranged from 12.41 to 117.77µm as determined by minimal Feret's diameter. Groups of small fibers (Figure 5.6.1 A and B, 1) were frequently found. Dense connective tissue (Figure 5.6.1 A, 2) and mononucleated cells (+ +) (Figure 5.6.1 B, 2) were present in perimysial regions. Inflammatory incidence ranged from no inflammatory infiltrate (0) to mild (+) (Figure 5.6.1 A and B) and moderate (+ +) (Figure 5.6.1 C and D) changes in both perimysial and endomysial regions. Fibers ranged from being intact, healthy appearing cells with peripherally located nuclei to fibers undergoing necrosis (Figure 5.6.1 A, 3). Minimal infiltration of adipose cells (±) was observed (Figure 5.6.1 A, 4).

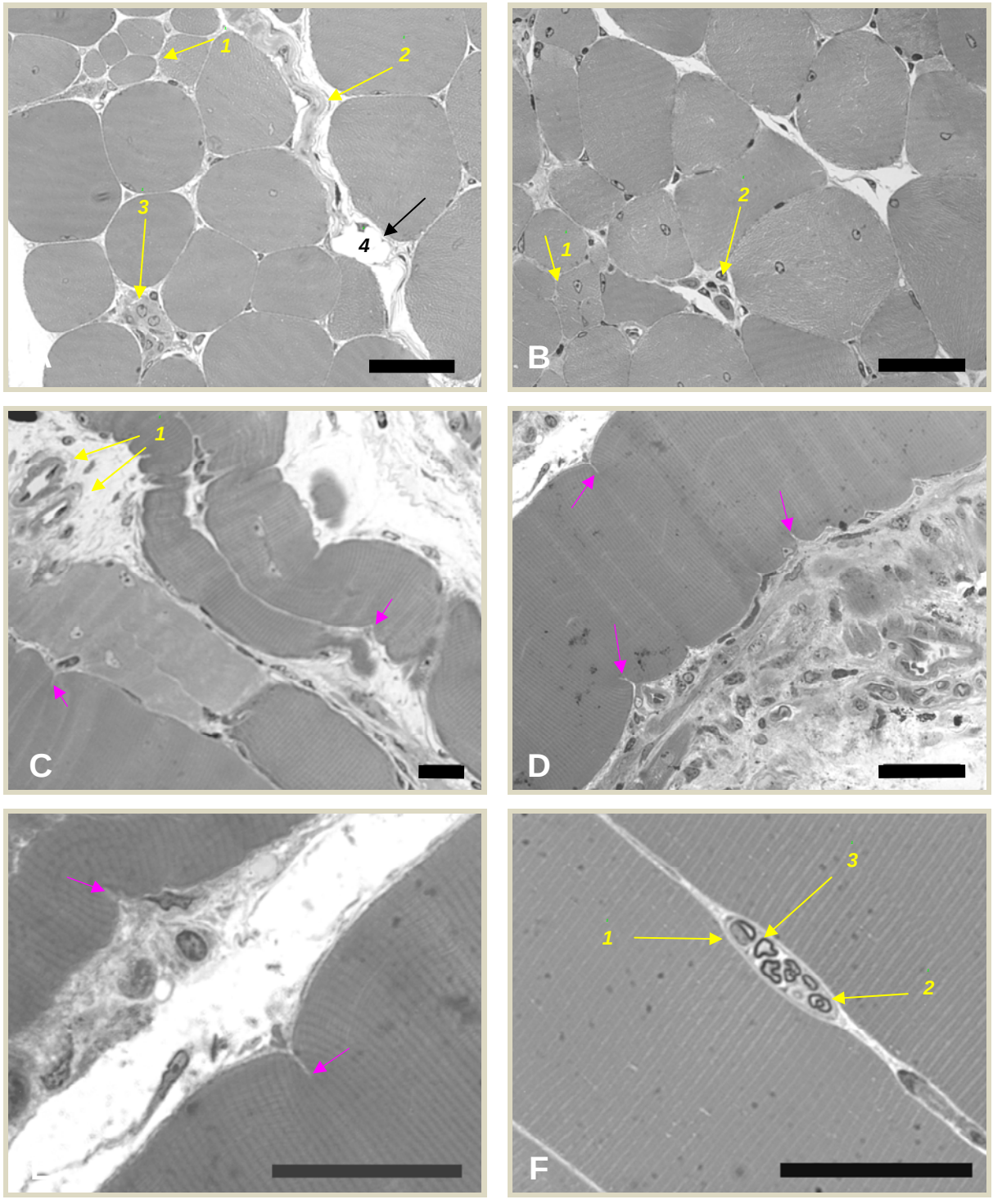

Figure 5.6.1: Quadriceps muscle sections from the 27 week-old SJL/J group treated with a low concentration of CoQ10. Sections were stained with Toluidine Blue O and Gill's Haematoxylin. A) Groups of small fibers (1) in a region with dense connective tissue (2) are present in perimysial areas. An ongoing necrotic process (3) and adipose infiltration (4) is present. B) A small group of two small fibers (1) are present with mononuclear cells (2) in the position where a fiber has undergone necrosis. C-E) Invaginations along the periphery of the fibers on a longitudinal section (pink arrows) are present. Blood vessels (C, 1) are present in the extracellular space. F) A nerve bundle (1) surrounded by a perineurium (2). Large meylinated fibers measuring up to 8µm in diameter probably represent proprioceptive afferents (3). Scale bars = 50µm

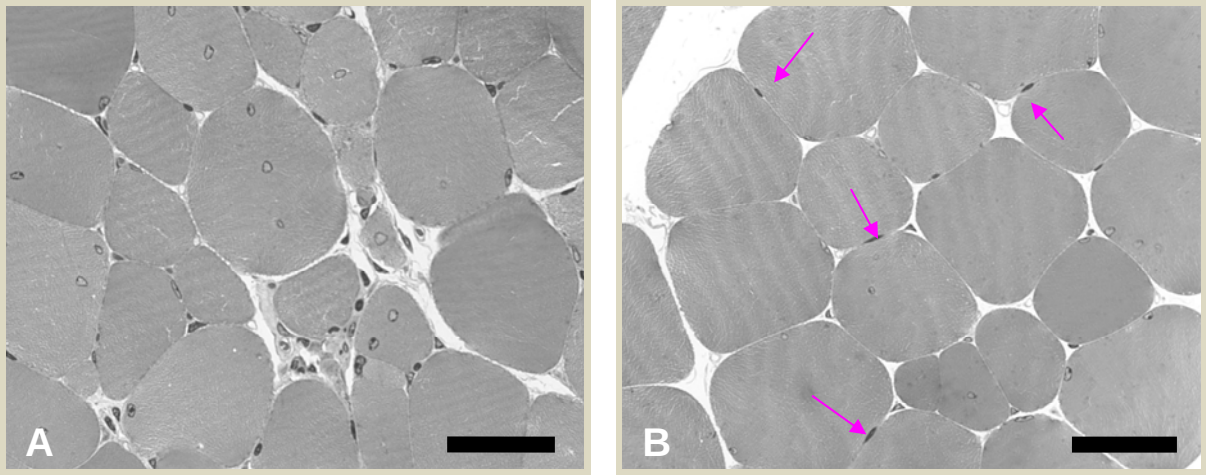

Figure 5.6.2: Quadriceps muscle sections from the 27 week-old SJL/J group treated with a low concentration of CoQ10. Sections were stained with Toluidine Blue O and Gill's Haematoxylin. A) Tissue from this group displays an incidence of 34.3% central nucleation. B) Nuclei, distinctly different in appearance from myonuclei, can be seen in this group, in intact fibers (pink arrows). The position of the nuclei fit that of satellite cells. Scale bars = 50µm

Longitudinal sections were mainly used as reference for orientation in the current study. Invaginations were observed along the periphery of the fibers (Figure 5.6.1 C, D and E, pink arrows) in some sections. These prominent indentations were of unknown origin, since no structure that could exert pressure to form the indentations could be detected in the vicinity. This incident was similar to that found in the 14 week-old group (Figure 5.3.2, C) and created the impression of fibers that are shrinking. Blood vessels (Figure 5.6.1 C, 1), dense connective tissue, and mononuclear cells were observed in the extracellular spaces of the endomysial regions in these sections. The specific incidence was observed in three different microscopic fields of one individual, while the other fibers appeared normal or necrotic in the longitudinal sections, but lacks these indentations. This observation remained to be further investigated on the ultrastructural level in chapter 6.

Nerve bundles (Figure 5.6.1 F, 1) with myelinated axons of Schwann cells were found quite frequently (+) in this group. Intramuscular nerves are seen in many muscle biopsies, but their presence as well as their orientation is a matter of chance. Intramuscular nerves are surrounded by a perineurium, a specialized structure made of flat cells with tight junctions (Figure 5.6.1 F, 2) (Carpenter and Karpati, 1984). Large myelinated fibers measuring up to 8µm in diameter probably represent proprioceptive afferents (Figure 5.6.1 F, 3) (Carpenter and Karpati, 1984).

Myonuclei in the central position of fibers (Figure 5.6.2 A) were found to be more abundant than in the resveratrol group, with an occurrence of 34.3%. Nuclei, distinctly different in appearance from myonuclei, were found in this group, in intact fibers (Figure 5.6.2 B, pink arrows). The position of the

nuclei fit that of satellite cells which are mononuclear cells found beneath the basal lamina of muscle fibers (Carpenter and Karpati, 1984). These cells are flat and somewhat elongated in the long axis of the muscle fiber. Their nuclei tend to contain darker clumped chromatin than myonuclei. When a muscle becomes necrotic, satellite cells are the source of the myoblasts (Figure 5.1) which regenerate the necrotic segment (Carpenter and Karpati, 1984). From a qualitative perspective; more intact cells were detected in this group compared to the positive control group samples (placebo), but less compared to the resveratrol group.

High CoQ10 group

Very little (±) (Figure 5.7 A) to mild (+) (Figure 5.7 B and C) and moderate (+ +) (Figure 5.7 D) degenerative and perimysial (Figure 5.7 B, C and E) inflammatory changes with endomysial involvement (Figure 5.7 A and D) were observed in animals treated with a high concentration (120mg/kg/day) CoQ10. As in the younger 14 week-old age control group, inflammatory changes, although more severe in this group, were found mostly in the perimysial regions where necrotic incidences (Figure 5.7 C and E, 1) could be detected.

A variation in fiber size was prominent, ranging from minimal Feret's diameter of 12.06 to 108.06µm (Figure 5.7 F). Nuclei in the central position of fibers were found in 22.9% of fibers analysed, which is distinctly lower than in the resveratrol and low CoQ10 groups. Markedly more myonuclei were detected in the peripheral position, and central nucleation was sparsely distributed in less and unaffected areas.

Numerous mononucleated cells (+) were present in infiltrate, indicating the presence of inflammatory incidence. Qualitative assessment indicated that fiber splitting (Figure 5.7 B and D, 1) occurred less frequently (±), compared to the resveratrol and low CoQ10 groups, and distinctly less frequently compared to the positive control group. Minimal adipose tissue infiltration (±) (Figure 5.7 D, 2) was seen in moderate (+ +) affected areas. Vacuolation (Figure 5.7 D, 3) were overall minimally (±) distributed in moderately (+ +) affected areas, while moth-eaten appearance (Figure 5.7 C, D and E, yellow asterisks) of cells was observed more frequently (+). No ring fibers were observed in the samples analysed from this group. A number of small capillaries were detected where they surrounded fibers, but did not indent them (Figure 5.7 A, B, C and E, white arrows). Nuclei, elongated, thin, and darkly stained, were also observed in the peripheral position in this group, in intact fibers (Figure 5.7 A, B, E and F, pink arrows). The position of the nuclei fit that of satellite cells. A number of nerve bundles located in the perimysial area were observed in some sections from this group (data not shown).

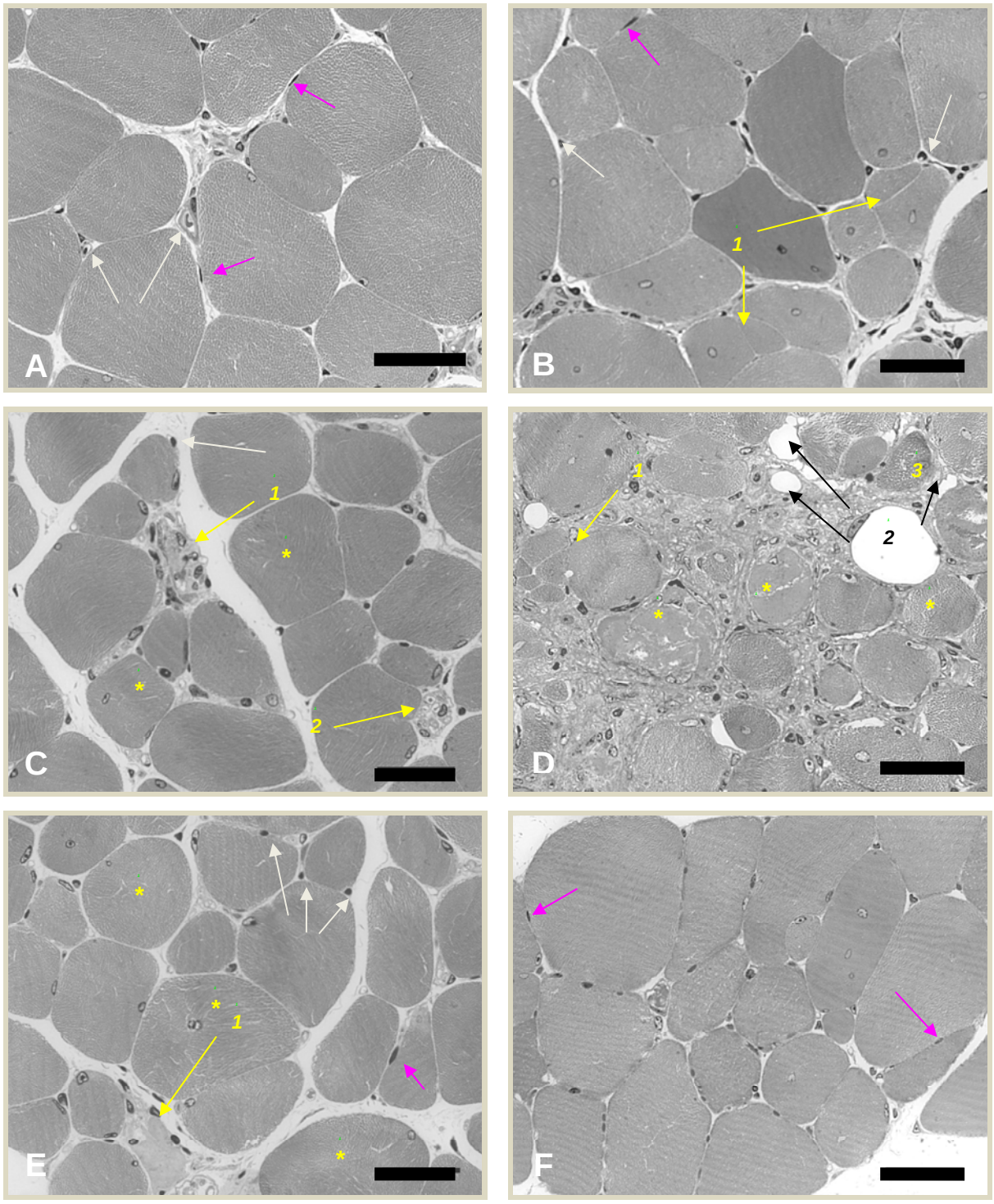

Figure 5.7: Quadriceps muscle sections from the 27 week-old SJL/J group treated with a high concentration of CoQ10. Sections were stained with Toluidine Blue O and Gill's Haematoxylin. Very little (A) to mild (B & C) and moderate (D) degeneration and perimysial (C & E, 1) inflammatory changes with endomysial involvement (A & D) are present. A number of small capillaries are present around fibers (white arrows). Fiber splitting (B & D, 1) is present, but less frequent. Mild adipose tissue infiltration (D, 2) is observed. Vacuolation (D, 3) is minimally distributed, while moth-eaten appearance (C, D & E, yellow asterisks) of cells is more frequent. F) Nuclei, distinctly different in appearance from myonuclei, are present (pink arrows; A, B, E & F). The position of the nuclei fit that of satellite cells Scale bars = 50µm

Resveratrol/CoQ10 combination group

Animals treated with a combination of resveratrol (60mg/kg/day) and CoQ10 (40mg/kg/day), showed minimal (±) (Figure 5.8 A and B) to mild (+) (Figure 5.7 C, D and E) degeneration and perimysial inflammatory changes with endomysial involvement (Figure 5.7 C, D and E). As in the high CoQ10 group, inflammatory changes were found mostly in the perimysial regions where necrotic incidences (± / +) (Figure 5.7 C and E, 1) could be detected extending into endomysial areas.

A variation in fiber size was prominent (Figure 5.8 A and B), ranging from minimal Feret's diameter of 13.17 to 108.10µm. Markedly more myonuclei were detected in the peripheral positions, and central nucleation was sparsely distributed (21.0% of all fibers analysed).

Numerous mononucleated cells (+) (Figure 5.8 C, D and E, yellow arrows) were present in affected areas. Fiber splitting (Figure 5.8 A, B and D, 1) occurred less frequently (±), compared to the positive control, resveratrol and low CoQ10 groups. Minimal adipose tissue infiltration (±) (Figure 5.8 D, 2) was observed. Ghost cells as a result of necrosis were detected (Figure 5.8 D, 3). Vacuolation (Figure 5.8 E, 1) was overall minimally distributed (±), while moth-eaten appearance (Figure 5.8 C and D, yellow asterisks) of cells was also markedly reduced compared to the findings in other groups. Ring fibers (Figure 5.8 E, 2) were observed in two samples of this group. The rings only affected part of the fibers, and did not form a complete ring. A few small capillaries were detected where they surrounded fibers. Elongated, thin, and darkly stained nuclei, that were possibly those of satellite cells were found in this group, in intact fibers (Figure 5.8 A and B, pink arrows), although in smaller numbers than in the high and low CoQ10 groups.

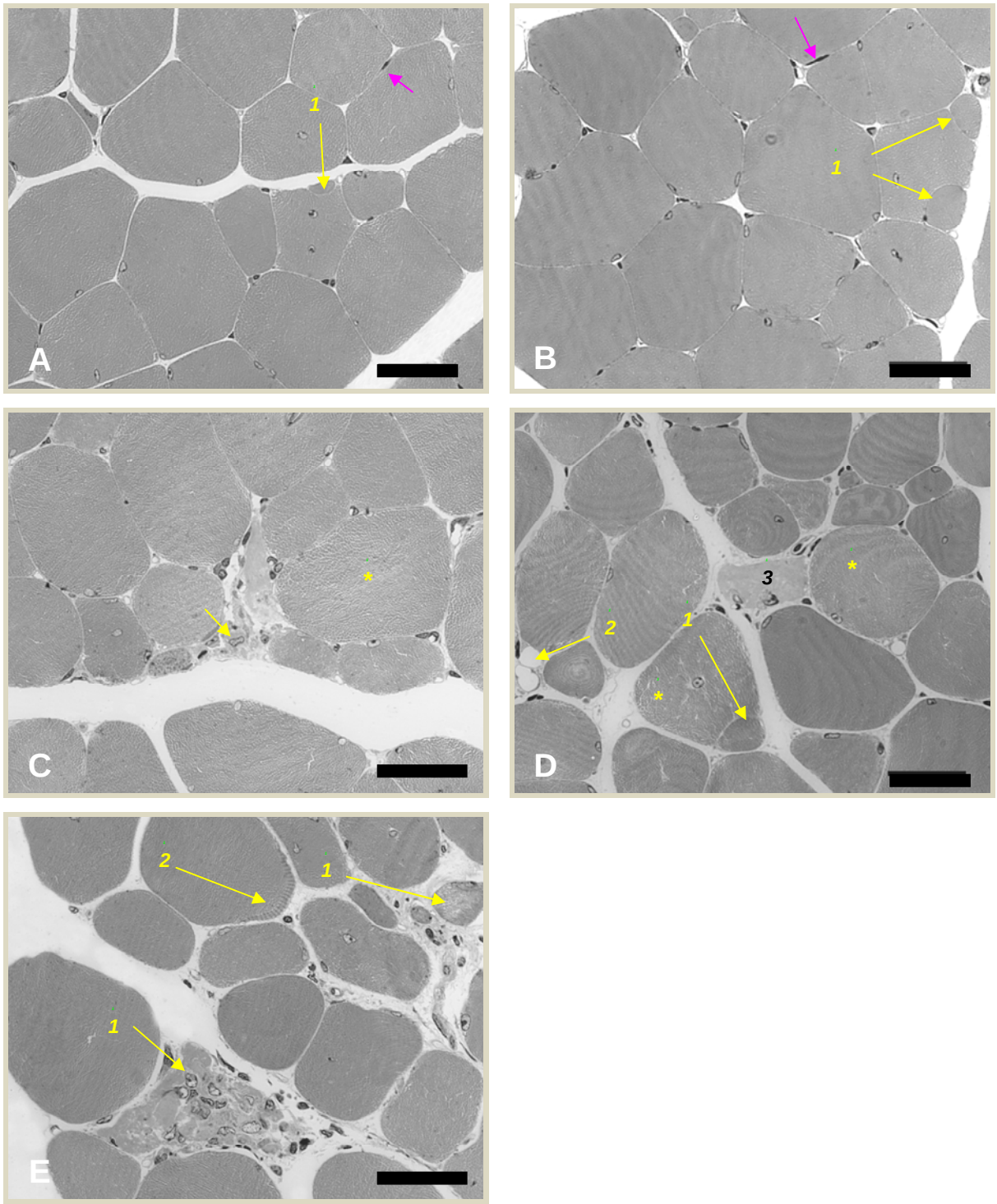

Figure 5.8: Quadriceps muscle sections from the 27 week-old SJL/J group treated with resveratrol/CoQ10 combination. Sections were stained with Toluidine Blue O and Gill's Haematoxylin. Minimal (A & B) to mild (C, D & E) degenerative and perimysial inflammatory changes with endomysial involvement (C, D & E) are observed in this group. Fiber splitting (A, B & D, 1) occurs less frequently. Minimal adipose tissue infiltration (D, 2) is present. Ghost cells as a result of necrosis (D, 3), vacuolation (E, 1), and moth-eaten appearance (C & D, yellow asterisks) of cells are minimally distributed. Mononucleated cells (C, D & E, yellow arrows) are present in affected areas. Ring fibers (E, 2) are observed, where it affected only part of the fiber. Nuclei, possibly belonging to satellite cells are observed in intact fibers (A & B, pink arrows). Scale bars = 50µm

Table 5.1 Summary and scoring of incidence of dystrophic processes in experimental groups

Age at termination (weeks)	27	27	27	27	27	14
Group / Changes	SJL/J Placebo	SJL/J Resveratrol	SJL/J (low) CoQ10	SJL/J (high) CoQ10	SJL/J Resveratrol + CoQ10	SJL/J No treatment
Fiber diameter range (µm)	11.82 – 99.01	10.12 – 117.90	12.41 – 117.77	12.06 – 108.06	13.17 – 108.10	15.98 – 112.34
% Central nuclei	35.4	31.6	34.3	22.9	21.0	8.8
Fiber splitting	+	+	±	±	±	±
Necrotic fibers / degeneration	+ +	+ / + +	+ / ++	+	± / +	±
Inflammatory infiltrate	+ +	+ / + +	+ / ++	0 / + / + +	+	±
Mononuclear cells (in extracellular spaces)	+ +	+	+ +	+	+	±
Ring fibers	Present	Present	Not detected	Not detected	Present	Not detected
Adipose infiltration	± / +	+	±	±	±	±
Vacuoles	+ / ++	+ / + +	+ / ++	±	±	±
Moth-eaten appearance	+ +	+ +	+ +	+	+	±
(**0**) = none; (**±**) = minimal; (**+**) = mild; (**+ +**) = moderate						

5.3.1.1 Necrosis

Necrosis was described by Carpenter, 2001 (a) as the death of a cell, where its inability to maintain homeostasis leads to its inevitable transition to debris. It is an irreversible phase during which the cell loses all function and viability (Carpenter and Karpati, 1984). Because of a muscle cell's multiplicity of nuclei, length and shape, it is possible for a segment of it to become necrotic while adjacent segments, termed stumps, survive (Carpenter and Karpati, 1984). Although a number of reports suggested that apoptosis can occur in skeletal muscle fibers, its status is not totally clear. At least in the cytoplasmic changes that accompany segmental death of a mature skeletal muscle cell, no distinction can be made between apoptosis and necrosis (Carpenter, 2001 a). Early stages of experimental necrosis, at the point where it begins, tend to show marked hypercontraction and tearing of myofibrils, resulting in a reticulated appearance (Figure 5.4.1, D).

Necrosis is often referred to as degeneration but this was thought to be an imprecise term that militates against exact pathological description (Carpenter and Karpati, 1984). Consistent with the literature (Kobayashi *et al.*, 2009), replacement of necrotic fibers by fatty (Figure 5.4.2, B) and fibrous (Figure 5.4.1, D) tissues was observed in the present study. Chiu and co-workers, 2009 have shown that reduced neutrophil recruitment in dysferlin-deficient muscle results in incomplete cycles

of regeneration. It was further reported that the inflammatory phase of muscle regeneration persisted beyond the stage where it was resolved in the control animals in their study. The team hypothesized that the persistent necrotic fibers provide foci for an ongoing inflammatory reaction, eventually directing cells towards a fibrotic fate.

The qualitative results of the present study suggest a reduction in necrotic incidence as well as in the amount of inflammatory foci in groups treated with the highest concentrations of antioxidants (high CoQ10 and resveratrol/CoQ10 combination groups) (Figures 5.7 and 5.8). These findings imply that the application of antioxidants interfere with the ongoing process responsible for initiation of necrosis, by an unidentified mechanism. It is nevertheless, tempting to speculate that the high dose antioxidants are most likely responsible for a reduction in metabolic disturbances, brought about by the ongoing inflammatory processes that were shown by Chiu's team. It is further suggested that these metabolic disturbances might also allow for accumulation of oxidative stress in the muscle, and that antioxidants scavenge these free radicals. This relief of oxidative stress insult will allow for the sufficient recruitment of anti-inflammatory cells, like neutrophils and macrophages. Thereby providing more effective clearance of necrotic fibers, and thus mediating more effective regeneration. The presence of oxidative stress in the SJL/J model will be further discussed in chapter 7 of the present study.

5.3.1.2 Inflammatory Infiltrate and the role of Macrophages

A study by Gallardo and co-workers, 2001, in patients with dysferlin-deficient dystrophy found that the predominant inflammatory cells were macrophages, which together with CD^{4+} T cells invaded degenerating fibers. True inflammatory cells are polymorphonuclear leucocytes, lymphocytes, plasma cells and monocytes (Carpenter and Karpati, 1984). Mononuclear cells seen in or around degenerative and/or necrotic muscle fibers of A/J and SJL/J mice was identified by Kobayashi and co-workers, 2009, as macrophages. Identification was based on their positive reaction for mouse F4/80 antigen, an antibody used to identify mouse macrophages.

Inflammatory cells which may be accompanied by increased fluid in the extracellular space (edema) may appear in muscle after various types of trauma or in inflammatory myopathies, (Carpenter and Karpati, 1984). Consistent with this statement, the findings of the present study revealed the presence of inflammatory cells surrounded by fluid, collectively termed inflammatory infiltrate in the present study, in and around fibers subjected to dystrophic changes Mitchell and co-workers, 1992, found the formation of new myotubes in SJL/J muscle after crush injury to be associated with efficient clearance of muscle debris by macrophages. Summan and co-workers, 2006, have shown

that clodronate liposome treatment, which targets mainly peripheral monocytes/macrophages result in a marked attenuation of the peak inflammatory response in injured muscle. Injured muscle was found to regenerate but the repair process was impaired by prolonged clearance of necrotic myofibers and a tendency for increased muscle fat accumulation (Summan *et al*., 2006).

Less inflammatory infiltrate was observed in muscle samples from the high CoQ10 and resveratrol/CoQ10 groups in the present study, compared to that observed in the positive control, resveratrol, and low CoQ10 groups.

5.3.1.3 Muscle Regeneration

Myogenesis involves the activation, proliferation and fusion (to form myotubes) of resident muscle precursor cells (myoblasts) that are normally quiescent on the surface of myofibres where they are termed satellite cells (Smythe *et al*., 2008). This process is tightly regulated by a complex interplay between various growth factors, and signalling and extracellular matrix molecules (Grounds, 2008). It involves a range of cell types including leukocytes, macrophages, and endothelial cells. Infiltration of damaged muscle by inflammatory cells is critical for the breakdown and removal of necrotic tissue, and when inflammation is prevented, the new muscle formation is impaired (Summan *et al*., 2006; Smythe *et al*., 2008; Chiu *et al*., 2009).

The ingrowth of new blood vessels (neovascularisation) is also required to support the process of new muscle formation (Smythe *et al*., 2008). The inflammatory and neovascular responses in injured skeletal muscle are dependent on changes in many components including the extracellular matrix (Grounds, 2008). The release of growth factors/cytokines from both muscle and non-muscle cell types (Smythe *et al*., 2008) promote these inflammatory and neovascular responses. A strong chemotactic response of leukocytes to skeletal muscle crush injury in SJL/J mice together with the weak response to uninjured muscle supported the concept that a local specific chemotactic factor is being generated at the site of injured muscle (Robertson *et al*., 1993).

Chiu and co-workers, 2009, identified a partial reduction in neutrophil recruitment associated with a reduction in macrophage recruitment in dysferlin-deficient muscle. This reduction in inflammatory response has been shown to cause a delay in clearance of necrotic fibers, leading to an ongoing inflammatory process, responsible for the dystrophic progression. In addition to its function in membrane repair, dysferlin has also been implicated in cytokine/chemokine release, following muscle injury (Chiu *et al*., 2009). Dysferlin deficiency is likely to be responsible for delayed regeneration of injured muscle fibers, resulting in the variation in fiber size observed in dysferlin-deficient muscle.

5.3.1.4 Small Fibers and Fiber Splitting

Small fibers may result from shrinkage or failure to grow, either primarily or after regeneration (Carpenter, 2001 a). Smallness refers to a reduced girth. An atrophic fiber can be regarded as a fiber measuring <20µm in diameter (Weller *et al.*, 1997), although not all fibers measuring <20µm are necessarily atrophic. The physiological, biochemical and molecular processes involved in storage and release of amino acids are collectively known as atrophy or wasting of muscle (Isfort, 2002). During atrophy, loss of a subset of proteins, including contractile proteins occurs (Isfort, 2002). Shrinkage is exemplified by the angular atrophic fibers of denervation, which tend to occur in groups (Carpenter, 2001 a). In diseases where necrosis is prevalent, as in the muscular dystrophies, small rounded fibers represent regenerants that have not been able to grow larger, because they do not have enough nuclei (Carpenter, 2001 a).

Fiber splitting refers to a group of small nested fibers with complementary contours (Figure 5.5.1, A 1) (Carpenter and Karpati, 1984). It might be debatable whether small fibers can result from longitudinal splitting of large fibers under normal conditions, but it is most probably the cause in the SJL/J mice, and more specifically dysferlinopathy (Figures 5.5.1, F; 5.6.1, A; 5.7.1, A). Split fibers are controversial. There is no consensus about their pathogenesis or even precise microscopic appearance. It has been suggested that hypertrophic fibers, due to a tendency towards structural abnormalities, might undergo fiber splitting (Carpenter and Karpati, 1984). Split fibers were frequently and without specific distribution, observed in all the groups in the present study. Carpenter and Karpati, 1984, described a split fiber as one which has a fissure extending from its periphery into its interior, consistent with what was seen on a transverse section in the present study (Figure 5.4.1, A, 1). Complete separation may result into what appear to be two distinct fibers whose contours are complementary to one another (Figure 5.7, B 1) (Carpenter and Karpati, 1984). The fissure may contain collagen and even a capillary. Some pathologists have been reported to use the term fiber splitting, as is the use in reporting the incidence in dysferlinopathy.

Four possible mechanisms have been suggested for fiber splitting or split fiber production (Carpenter and Karpati, 1984): Firstly, hypertrophied fibers under stress undergo actual cleavage, developing an invagination of the surface membrane which partially or completely divides them. A second possibility is the activation of satellite cells in the absence of muscle fiber necrosis. Thirdly, atrophic denervated fibers not only become angular but can present quite bizarre shapes. If such a fiber was reinnervated, and subsequently grew to a large size, it might assume a split appearance. A fourth mechanism appears to actually operate in producing small grouped nested fibers and forking. After necrosis the regenerating myotubes within a single basal lamina may fail to undergo lateral fusion

with one another, but they may fuse with the surviving stump, thus giving rise to a fiber with one or more forks (Carpenter and Karpati, 1984).

Totsuka and co-workers, 1998, suggested that splitting and/or fusion in dystrophic muscle may represent compensatory phenomena related to defective growth. From the current histopathology data it is more likely that the first mechanism proposed by Carpenter and Karpati, 1984, is involved in fiber splitting in dysferlinopathy. The large fiber size variation and a relative prominent shift towards fibers with a larger minimal Feret's diameter in SJL/J mice suggest that hypertrophied fibers under stress conditions may develop an invagination of the surface membrane. The invagination proceeds to complete separation, resulting in two or more small fibers. Totsuka and co-workers, 1998, showed that the summed area of post-splitting daughter fibers was almost the same as that of the parent fiber, indicating that the cross-sectional area is conserved after splitting. This statement is consistent with the split fibers observed in the present study. More than one mechanism might be involved. However, it has been shown that fiber splitting does not appear to be associated with loss of fiber content (Totsuka *et al*., 1998). Totsuka and co-workers therefore suggested that it may appear as a compensatory mechanism rather than a degenerative change. Discussion of the fiber size variation in SJL/J mice later in this chapter will provide more insight to this ambiguity.

5.3.1.5 Ring Fibers

A subset of the myofibrils, instead of extending parallel to the long axis of the muscle fiber, may be found circling or spiralling around the long axis (Carpenter and Karpati, 1984; Schotland *et al*., 1966). These structures have been termed ring myofibrils, spiral annulets, or ringbinden (Carpenter and Karpati, 1984), and they are not contraction band artefacts due to acid fixation or other cause (Schotland *et al*., 1966). Ring myofibrils are newly formed structures arising in muscle fibers which were normal, until their growth pattern was modified by the pathological process (Schotland *et al*., 1966).

The myofibrils in the center of such fibers tend to look normal. Sometimes the ring myofibrils may dip towards the center of the muscle and be sandwiched between normally oriented myofibrils. The fibers affected by the phenomenon are termed ring fibers (Carpenter and Karpati, 1984). The rings may be composed of a single myofibril, or more commonly can be 4 to 5 myofibrils thick. Occasionally much thicker rings may be found. Carpenter and Karpati, 1984, reported that elements of sarcoplasmic reticulum and T-tubules may be seen among the ring myofibrils and that mitochondria tend to be absent from them.

Affected myofibrils tend to be thinner than normal myofibrils (Carpenter and Karpati, 1984). Carpenter and Karpati, 1984 stated that ring fibers can be seen in the majority of myotonic dystrophy cases, and in over half of the cases of limb girdle dystrophy. It has been denoted conceivable that these structures are the result of disorderly myofibrillar protein synthesis or from a disorder of the cytoskeleton (Carpenter and Karpati, 1984). Bethlem and Van Wijngaarden, 1963 suggested that ring myofibrils may also branch from the ring, penetrate the muscle fiber and rejoin the aberrant myofibrils on the opposite side. This description correlates with what was termed snake coils, by Carpenter and Karpati, 1984. It was described to be represented by a braided appearance of the myofibrils on semithin resin sections and to occur in hypertrophied fibers in a variety of diseases, like denervation atrophy, and limb girdle dystrophy. A disorder of the cytoskeleton was suggested to be involved (Carpenter and Karpati, 1984).

Snake coils were found in the present study. Figures 5.4.2, A; 5.5.1 C, 2 and E, 1 showed that the myofibrils assume a streaming pattern, and appear distorted on semithin resin sections. This snake coil structures were also detected in fibers not displaying ring myofibrils on semithin resin sections (Figures 5.5.2 B,1 and 5.6.1 C2, and E1) in the present study. Schotland and co-workers, 1966, reported an electron microscopic study that confirmed the presence of peripheral circumferential ring myofibrils oriented in a plane at right angles to the muscle fiber. The presence of ring fibers in the dysferlinopathies has previously been described by others (Selcen *et al*., 2001; Comerlato *et al*., 2005; Pongpakdee *et al*., 2007; Liewluck *et al*., 2009). In the present study ring fibers have been identified, possibly for the first time, in the SJL/J mouse model (Figures 5.5.2 A, 1; 5.6.1 D, 1; 5.9 E, 2). Because of the rareness of these structures, it is impossible to draw any conclusions as to what role the administration of antioxidants in the present study could have or not have played in their formation and appearance.

5.3.1.6 Connective Tissue

Collagen is recognized to have several important functions as a structural component of all muscular tissues (Mayne, 1982). This connective tissue forms the linkages between the muscle and its associated connective tissues such as tendon or fascia. Collagen is the fibrillar component of the cell-to-cell connections which are present between individual muscle cells and between the muscle cells and neighbouring arteries, arterioles, veins, venules and capillaries (Figure 5.3.2 A and B) (Copenhaver *et al*., 1978).

Normally, so little collagen is present between muscle fibers that it is only visible by electron microscopy. An exception is in the region of neuromuscular junctions, where a small amount of

collagen tends to encircle muscle fibers (Carpenter, 2001 a). Muscle that has been severely damaged tends to show increased endomysial connective tissue (Figure 5.6.1 A, 2), usually in the form of tether, loose, randomly oriented collagen. In Duchenne and Becker dystrophy, the connective tissue proliferation, which begins to occur early, is distinctive, consisting of discrete dense bundles of collagen laid down parallel to the muscle fibers (Carpenter, 2001 a). This might be associated with irreversible joint contractures often observed in these patients (Carpenter, 2001 b). Carpenter, 2001 (a), reported that this pattern is also seen in some biopsies from patients with a limb girdle syndrome. In the present study, the finding of collagen parallel to muscle fibers (Figure 5.5.1 F,2) and in the endomysial (Figure 5.6.1 A, 2) regions in SJL/J mouse muscle, suggest the above findings by Carpenter, 2001 (a) are also true for the SJL/J dysferlinopathy animal model. The observation suggests that the excessive deposition of collagen in dysferlinopathies might also result in joint contractures seen in these patients at later stages of disease.

5.3.1.7 CAPILLARIES

Capillary density around some fibers has been shown to be increased in inclusion body myositis (Carpenter and Karpati, 1984). The number of capillaries in most cases of inclusion body myositis appears increased over normal. To some extent this increase reflects the atrophy and loss of muscle fibers. Other authors found fibers which appeared to have an excess of mitochondria to be indented by an unusually large number of capillaries (up to twelve) on cross section of inclusion body myositis samples (Carpenter and Karpati, 1984). The maintenance of higher vascularisation may be related to the frequent presence of ragged red fibers with abnormal mitochondria (Carpenter and Karpati, 1984).

Microvessel density has been shown to decrease with age in both, golden retriever muscular dystrophy (GRMD) dogs, and healthy control subjects (Nguyen F *et al*., 2005). Nguyen, F and co-workers, 2005 have demonstrated that fibrosis, the hallmark of muscle pathology in DMD boys and GRMD dogs, seems to be the major factor influencing mircrovascular architecture in skeletal muscles. The increasing extent of connective tissue correlated with lower microvessel density and longer intercappillary distance. This might create a physical barrier between the capillary contour and the myofiber membrane (Nguyen F *et al*., 2005). It is therefore a matter of concern that endomysial fibrosis might compromise intravascular therapeutic strategies performed in later stage muscular dystrophy.

In the present study, capillaries surrounding and indenting fibers that correlate with that found by Carpenter and Karpati, 1984, in inclusion body myopathy, were prominent in the 14 week-old SJL/J

mice (Figure 5.3.2 D). It was only minimally present in the resveratrol group (Figure 5.5.2 B, 1). Considering the prevalence of capillaries in the younger SJL/J mice, it is probably suggestive of higher vascularisation, associated with the increase in inflammatory incidence, and the higher demand of effective inflammatory cell transportation to the site of inflammation. It is furthermore possible, that as the inflammation starts to increase vascularisation is activated as compensatory mechanism in order to supply more immune cells to the site for more effective cleanup. The fact that fewer capillaries were observed in 27 week-old SJL/J mice suggest that this mechanism is less active after a certain age or disease stage. Smythe and co-workers, 2008, reported that the release of growth factors/cytokines from both muscle and non-muscle cell types are required for inflammatory and neovascular responses. It is therefore possible that older SJL/J mice lack sufficient chemotaxis for recruitment of these responses.

5.3.1.8 CENTRONUCLEATION

Displacement of nuclei from their normal subsarcolemmal position is the most common abnormality involving nuclei (Carpenter, 2001 a). Since semithin resin sections are so thin (1µm), they reveal far fewer nuclei than cryostat sections. Literature on histopathology in dysferlinopathy repetitively reports on nuclei detected in the central position of muscle fibers. While numerous reports suggested that nuclei in the central position of a fiber are indicative of regeneration, Totsuka and co-workers, 1998, reported that centronucleation is not a marker for regenerated fibers. Their team have demonstrated in dy/dy dystrophic mice that centronucleated fibers may otherwise be essentially normal.

Totsuka and co-workers, 1998, speculated that peripheral myonuclei may be restrained by the proximity of membranous structures in fibers. Central nuclei might therefore be more active than their peripheral counterparts, playing some important role in the growth and homeostasis of muscle. It is noteworthy that central nuclei (in general less than 1%) may also be observed in fibers of normal mammalian muscles (Totsuka *et al*., 1998).

In the present study, more than 35% of fibers analysed from the positive control group displayed nuclei in the central position of quadriceps muscle fibers, compared to the 0.8% of the negative control group, and 8.8% in the age control group (Figure 5.9). The numbers in the resveratrol and low CoQ10 groups compared with that of the positive control, at 31.6%, and 34.3%, respectively. The high CoQ10 and resveratrol/CoQ10 combination groups displayed markedly lower numbers compared to the positive control, resveratrol and low CoQ10 groups at 22.9% and 21%, respectively.

High levels of antioxidant supplementation in SJL/J mice have caused a decrease in the number of fibers with nuclei in the central position in quadriceps muscle.

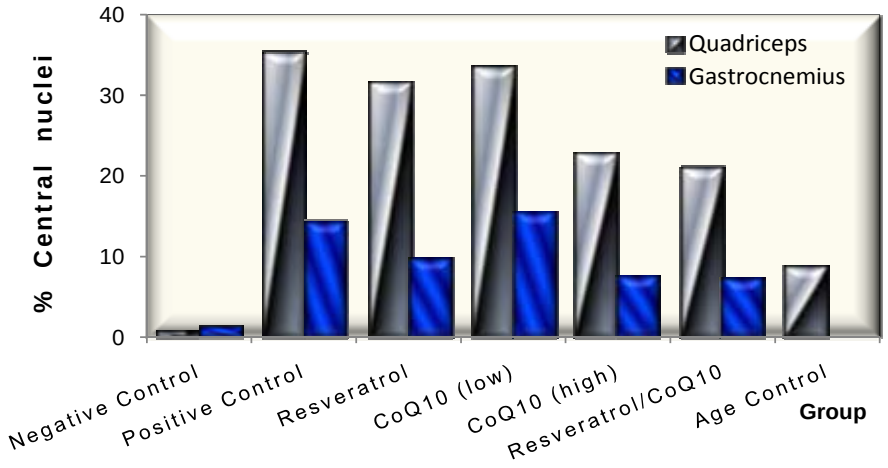

Figure 5.9: Percentage central nuclei in gastrocnemius and quadriceps muscle fibers.

Figure 5.9 shows the distinct lower number of nuclei in the central position of less affected gastrocnemius fibers from the same animals, compared to the quadriceps fibers. The highest numbers were found in the positive and low CoQ10 groups, at 14.4% and 15.5%, respectively. The resveratrol, high CoQ10 and resveratrol/CoQ10 combination groups displayed less than half this numbers.

From the present study, it can be suggested, that even if central nuclei is not a marker of regeneration, it is less frequent in muscle less affected by the ongoing dystrophic processes. It can be suggested that the mechanism responsible for centronucleation are affected by dysferlin-deficiency. From the results it is evident that high dose antioxidant supplementation in SJL/J mice, markedly reduces the manifestation of central nuclei in both quadriceps and gastrocnemius muscle fibers.

5.3.2 Morphometric Findings

Certain procedures such as measurement of the perimeter or the cross-sectional area of a fiber are mainly influenced by the plane of sectioning (Briguet *et al*., 2004). These authors described a method and provided reference values for the rapid, quantitative and reliable measurement of a relevant histological parameter of the dystrophic muscle in the mdx-mouse. The method relied on the determination of the muscle fiber size using the minimal Feret's diameter of a muscle fiber as seen in cross-section. The minimal Feret's diameter is a geometrical parameter that is frequently used for morphometric analysis (Nguyen F *et al*., 2005; Rouger *et al*., 2007; Grounds *et al*., 2008;

Steen *et al*., 2009), and is defined as the minimum distance between parallel tangents at opposing borders of the muscle fiber (Briguet *et al*., 2004).

Unlike other parameters to determine muscle fiber size, the minimal Feret's diameter parameter is very robust against experimental errors such as the orientation of sectioning angle (Briguet *et al*., 2004). Moreover, it reliably discriminates between dystrophic and normal phenotypes in a representative set of muscles.

The minimal Feret's diameter determined for all fibers of a specific muscle cross section were given as mean, minimum, and maximum, where the mean values were compared between groups for quadriceps (Figures 5.10 and 5.11) and gastrocnemius muscles (Figures 5.12 and 5.13), respectively. Measurements were also compared between the two muscles (Figure 5.14). Together with the percentage of fibers with centralized nuclei, this information is considered a reliable histological assessment of the pathology associated with dystrophin-deficiency (Briguet *et al*., 2004), and was therefore chosen for the quantitative component of the histological assessment of the pathology associated with dysferlin-deficiency in the SJL/J mouse model of the present study. A summary of the differences in fiber diameter is given in Table 5.3.

Comparison of Fiber Diameter in Quadriceps Muscle Fibers

An equal sample size of 500 measurements existed in each experimental group, therefore the assumption of equal variance was ignored. The parametric one-way ANOVA test could not be utilized to assess if there was any difference between the minimal Feret's diameters of experimental groups. The reason being the data did not assume a normal distribution. The fiber diameter of quadriceps muscle fibers was therefore compared via the non-parametric Kruskal-Wallis one-way test. This test revealed that a significant difference ($P < 0.000001$) existed between two or more of the compared six experimental groups (Figure 5.10). Tukey-Kramer Multiple Comparison tests were run, once again as *pos hoc* tests, in order to elucidate where this significant difference lay.

The age control group displayed a significant smaller mean minimal Feret's diameter compared to all the other groups. Fibers from the resveratrol group were significantly smaller in their diameter than that of the negative control group. The positive control and resveratrol groups' fibers displayed a significantly smaller mean minimal Feret's diameter compared to both CoQ10 groups. The diameter distribution (Figure 5.11) in both the CoQ10 groups displayed a peak size between 50 and 60µm, and thereafter a gradual extension of the skirt towards larger diameters, in contrast to the peak range observed in the positive control and resveratrol groups at 60 to 70µm and 40 to 50µm, respectively.

In the resveratrol group the percentage of fibers in the range larger than 50µm (≈56.1%) is proportional to the percentage of fibers smaller than 60µm (≈51.8%) in the positive control group. Although these two groups displayed very similar mean minimal diameters, the size tendency is towards different directions where the positive control fibers displayed a tendency towards a smaller fiber size, while the resveratrol group fibers displayed a tendency towards a larger fiber size. This might implicate that antioxidant supplementation with resveratrol facilitate the maturation of regenerated fibers.

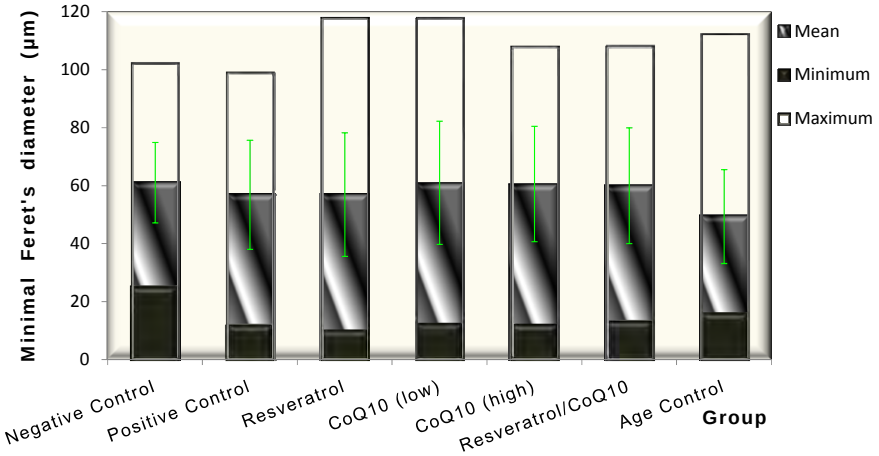

Figure 5.10: Minimum, mean (middle part of bars) and maximum minimal Feret's diameter of fibers measured in Quadriceps muscle tissue, with error bars representing the standard deviation (SD).

The resveratrol/CoQ10 combination group did not differ significantly in its mean minimal Feret's diameter to any other group, except the age control group. The data suggests a significant increase in mean minimal Feret's diameter of muscle fibers in quadriceps muscles of SJL/J mice from age 14 to 27 weeks. The small diameters in 14 week-old SJL/J mice is in relation to little disruption at the cellular level, as displayed by histopathology analysis (Figures 5.3.1 and 5.3.2), whereas the larger diameters in older SJL/J mice is in relation to a much disrupted phenotype at the cellular level of 27 week-old mice (Figures 5.4.1 and 5.4.2).

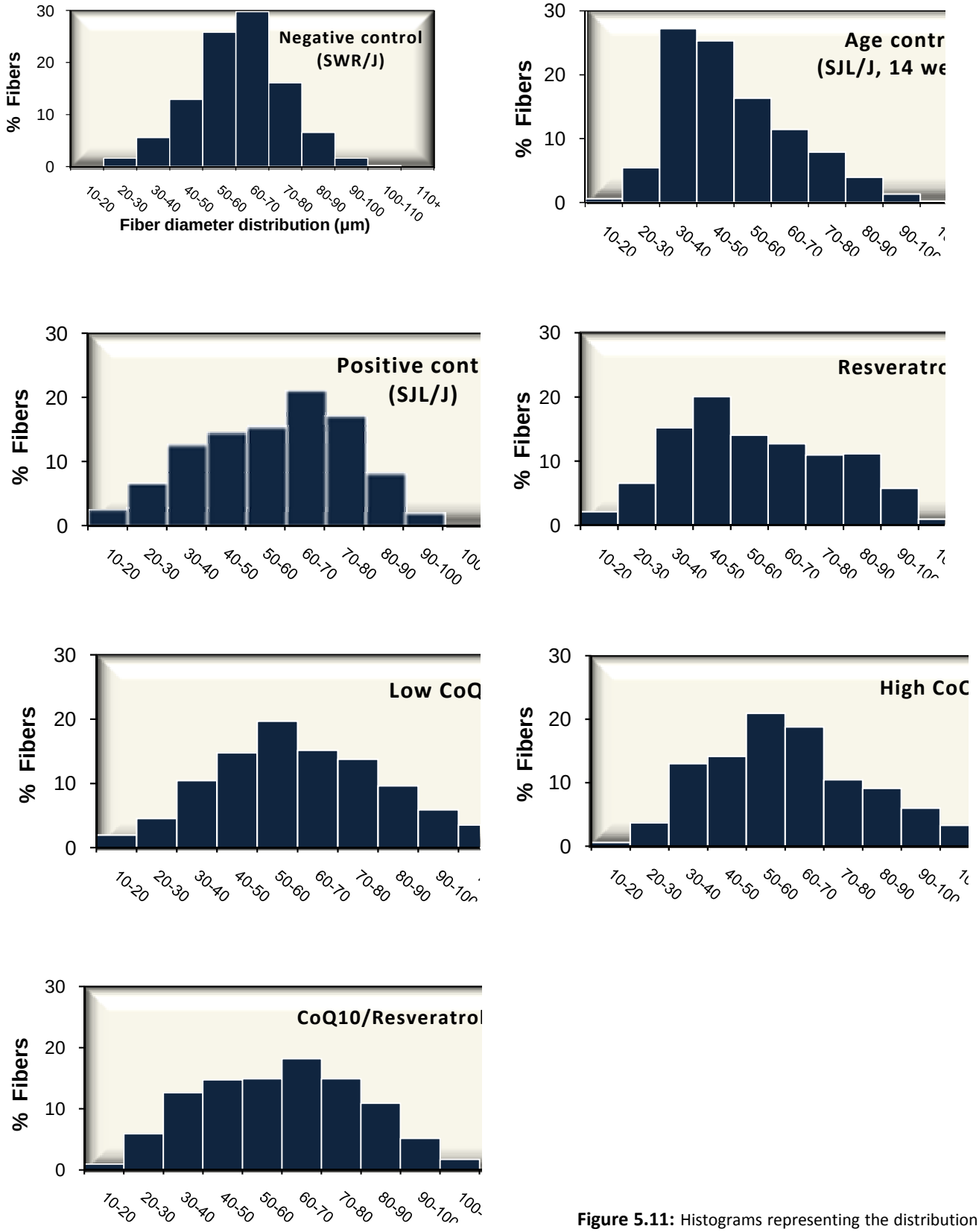

Figure 5.11: Histograms representing the distribution of mean fiber diameters in quadriceps muscles of experimental groups.

The data further suggests that the mean minimal Feret's diameter of all experimental groups treated with an antioxidant or combination thereof, did not differ significantly from that of the negative control group. However, in some groups (age control, resveratrol, low CoQ10 and high CoQ10) the fiber size distribution histograms (Figure 5.11) displayed a peak shift towards smaller fiber size, but with a larger number of fibers towards larger fiber sizes, compared to the positive control group. This observation strengthens the notion that antioxidant supplementation may afford maturation of regenerated fibers in older SJL/J mice.

Comparison of Fiber Diameter in Gastrocnemius Muscle Fibers

As equal sample size of 500 measurements, existed in each experimental group the assumption of equal variance was ignored. The parametric one-way ANOVA test could not be utilized to assess if there was any difference between the minimal Feret's diameters of experimental groups. The reason is the data did not assume a normal distribution. As a result, the gastrocnemius fiber diameters were compared via the non-parametric Kruskal-Wallis one-way test. This test revealed that a significant difference ($P < 0.000001$) existed between two or more of the six groups (negative control, positive control, resveratrol, low CoQ10, High CoQ10, and resveratrol/CoQ10 combination groups) compared (Figure 5.12). Tukey-Kramer Multiple Comparison tests were run in order to elucidate where this difference lay.

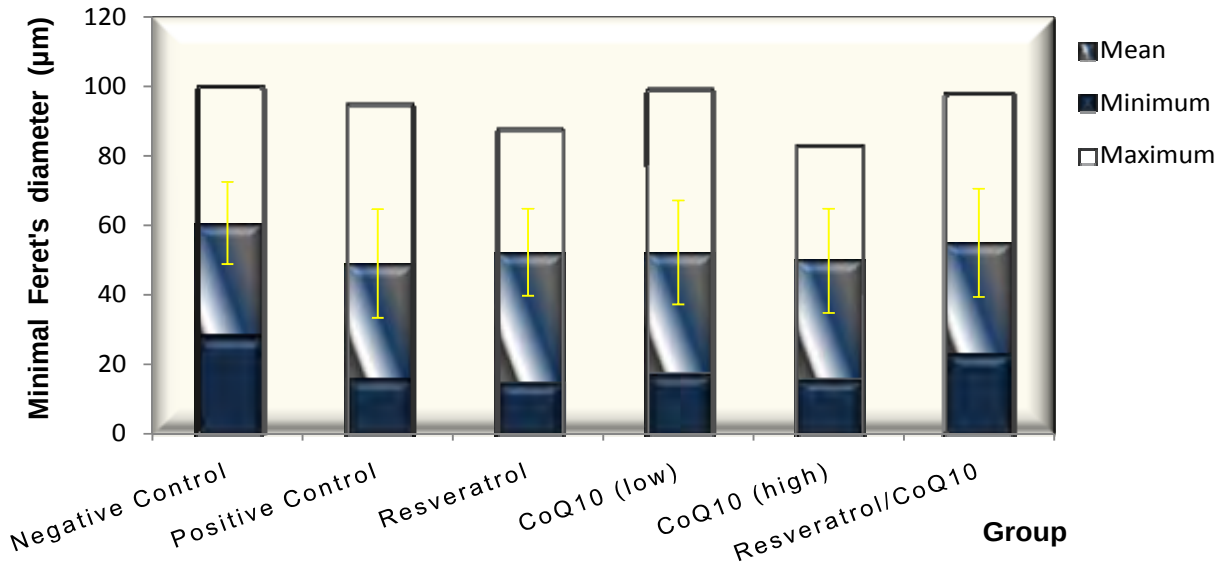

Figure 5.12: Minimum, mean (middle part of bars) and maximum minimal Feret's diameter of fibers measured in Gastrocnemius muscle tissue, with error bars representing the standard deviation (SD).

Mean minimal Feret's diameter in gastrocnemius fibers from the negative control group was significantly larger in comparison to all the other groups. When looking at the distribution of the data (Figure 5.13) in the negative control group, peak sizes occur at 60 to 70µm, with a rapid elevation of the skirt from smaller size towards the peak, followed by an even sharper drop towards larger diameters. The resveratrol group displayed the closest similarity in its fiber size distribution to the negative control group, with the exception of the peak shift towards 50 to 60µm.

The positive control group displayed a significantly smaller diameter to all groups except to the high CoQ10 group. Peak values in the positive control group were observed in the 40 to 50µm range, followed by a more gradual extension of the skirt towards larger diameters (Figure 5.13). The high CoQ10 group showed peak sizes in the 50 to 60µm range, followed by a very rapid and sharp drop towards a maximum of 80 to 90µm.

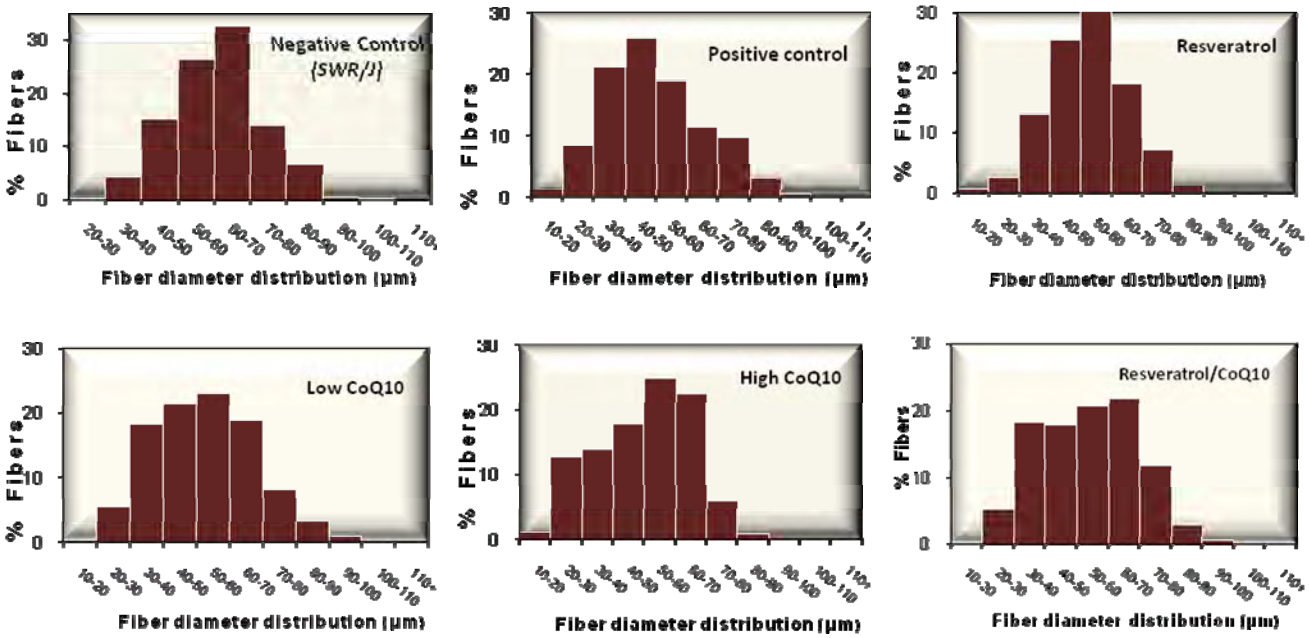

Figure 5.13: Histograms representing the distribution of mean fiber diameters of gastrocnemius muscles of experimental groups.

The increased proportion of fibers with diameters between 20 and 60µm in the high CoQ10 and resveratrol/CoQ10 combination groups were markedly different from that observed in other groups (Figure 5.13). The mean minimal Feret's diameter of the high CoQ10 group displayed significantly lower values than that observed in the resveratrol/CoQ10 combination group.

The values measured in the gastrocnemius muscle displayed closest similarity in mean minimal Feret's diameters to the age control group's quadriceps fibers. This observation suggests that the fiber condition in gastrocnemius muscle show similarity to that of quadriceps muscle in a younger phenotype.

Table 5.2 Summary of the mean minimal Feret's diameter of muscle fibers from gastrocnemius and quadriceps muscles, the diameter range, the amount of fibers analysed and the number of fibers that displayed central nucleation

Group	Quadriceps				Gastrocnemius			
	Mean minimal Feret's diameter ± SD (µm)	Number of cells measured	Number of central nuclei	Diameter range (µm)	Mean minimal Feret's diameter ± SD (µm)	Number of cells measured	Number of central nuclei	Diameter range (µm)
Negative control SWR/J mice	61.07 ± 13.85	504	4	24.81 – 102.19	60.65 ± 11.81	504	7	28.05 – 100.48
Positive control SJL/J, Placebo	56.90 ± 18.86	539	191	11.82 – 99.01	49.02 ± 15.64	514	74	15.68 – 95.21
Resveratrol	56.94 ± 21.31	519	164	10.12 – 117.90	52.25 ± 12.55	543	53	14.56 – 88.05
Low CoQ10	61.04 ± 21.21	508	174	12.41 – 117.77	52.20 ± 14.98	521	81	17.02 – 99.59
High CoQ10	60.63 ± 19.90	516	118	12.06 – 108.06	49.77 ± 15.03	500	38	15.5 – 83.47
Resveratrol/CoQ10 combination	60.02 ± 19.96	523	110	13.17 – 108.10	54.94 ± 15.57	574	42	22.81 – 97.87
Age control 14 week-old; SJL/J	49.38 ± 16.22	533	47	15.98 – 112.34				

Comparison of Fiber Diameter between Quadriceps and Gastrocnemius Fibers

The minimal Feret's diameter of gastrocnemius and quadriceps muscle fibers was compared within each group (Figure 5.14). The assumption of equal variance was ignored due to the comparison of equally sized samples. The parametric comparison test, the T-test, could only be utilized when comparing the different muscles' minimal Feret's fiber diameters in the negative control group as only in this situation did the assessed data assume a normal distribution pattern. In the case of all the other assessed groups, the data in one or both of the assessed muscle types did not assume a normal distribution and thus resulted in the non-parametric Mann-Whitney U test being utilized for comparison instead.

Table 5.3 Summary of the statistical comparison of fiber size between different groups and different muscles

Group		Morphometric findings (minimal Feret's diameter)				
		Quadriceps ($P < 0.000001$)		Gastrocnemius ($P < 0.000001$)		Quadriceps vs Gastrocnemius
		*Significantly **larger** than:*	*Significantly **smaller** than:*	*Significantly **larger** than:*	*Significantly **smaller** than:*	Quadriceps significantly larger than gastrocnemius in all groups, but the negative control
Control	**Negative Control (SWR/J)**	Age control, Positive control; Resveratrol	none	All groups	none	No significant difference ($P = 0.604177$)
Control	**Positive Control (SJL/J_27 weeks)**	Age control	Negative control; Low CoQ10; High CoQ10	none	Negative control; Resveratrol; Low CoQ10; Resveratrol/CoQ10	$P < 0.000001$
Control	**Age Control (SJL/J_14 weeks)**	none	All groups	none	Negative control	-
Experimental	**Resveratrol**	Age control	Negative control; Low CoQ10; High CoQ10	none	Negative control	$P = 0.006181$
Experimental	**Low CoQ10**	Age control; Positive control; Resveratrol	none	none	Negative control	$P < 0.000001$
Experimental	**High CoQ10**	Age control; Positive control; Resveratrol	none	none	Negative control; Resveratrol/CoQ10	$P < 0.000001$
Experimental	**Resveratrol/CoQ10 combination**	Age control	none	none	Negative control	$P = 0.000034$

For each of the other experimental groups the Mann-Whitney U test revealed that there was a significant difference between the two muscle types' fiber diameters (positive control group, $P < 0.000001$; resveratrol group, $P = 0.006181$; low CoQ10 group, $P < 0.000001$; high CoQ10 group, $P < 0.000001$; resveratrol/CoQ10 combination group, $P = 0.000034$)

The minimal Feret's diameters of quadriceps muscle fibers were in all instances found to be significantly greater than that of the gastrocnemius muscle fibers. This is consistent with the suggestion that gastrocnemius fibers are phenotypically similar to quadriceps fibers observed in the age control group.

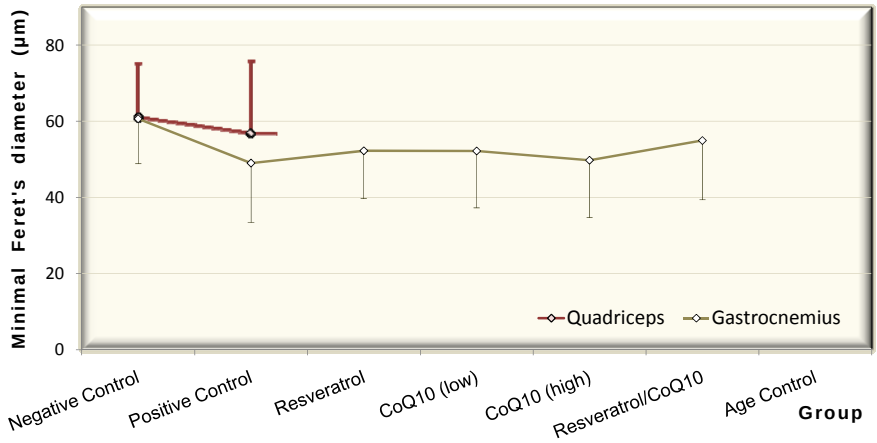

Figure 5.14: Relationship between mean minimal Feret's diameters measured in quadriceps muscle fibers and gastrocnemius muscle fibers. The error bars represent the standard deviation (SD).

5.3.3 Fiber Size

5.3.3.1 Variation in Quadriceps Muscle Fibers

The variation in fiber size was found to be the largest in the low CoQ10 and resveratrol groups, where variation is indicated by the range between minimum and maximum minimal Feret's diameter in a group (Table 5.2). A similar variation was observed in the age control group, although the minimum value was higher than that in older mice and the mean lower. The greatest number of fibers in the age control group displayed sizes smaller than 60µm (which is where fiber size in the negative control group peaked). The peak values occurred at smaller diameters in the age control group, while a very small number of fibers measured up to 110µm, and even larger. The reason for this could be that the active phase of the disease is setting in around this age, whereas muscle deterioration is not yet evident at cellular level. A low occurrence of fiber splitting was observed, and a large number of fibers were still in the process of maturation.

A stable fiber size distribution pattern was observed in the negative control group. The small variation in the negative control group indicates healthy, growing fibers. A larger proportion of fibers were found to be of intermediate size (peak values between 60 and 70µm), equally distributed between actively maturing fibers. The skirt of the histogram from the negative control group showed a firm but gradual increase towards the peak, and a slightly steeper, decline towards larger diameters (Figure 5.11). A very small number of fibers were larger than 100µm in diameter.

The small variation in the positive control group might indicate the disability of fibers to reach larger diameters because of the ongoing dystrophic process preventing maturation of myofibers. The continuous occurrence of fiber splitting observed from the histopathological picture in this group is contributing to this variation. From the histogram on fiber size distribution (Figure 5.11), it is clear that there is no tendency towards hypertrophy in this group, while a larger proportion of fibers displayed sizes smaller than the peak diameters. The tendency towards smaller diameter predominance in the positive control group can result from a combination of active regeneration with a lack of maturation, atrophy of fibers, and fiber splitting. When comparing the qualitative histopathology assessment of fiber splitting with the minimum minimal Feret's diameters over all the groups, it shows that the lower the incidence of fiber splitting, the higher the minimum diameter of fibers.

Fibers from both the resveratrol and low CoQ10 groups, showed a predominance towards larger fiber size compared to the positive and age control groups. The highest incidence of large fiber diameter, >110µm, was also recorded in these two groups. This data suggests that the application of antioxidant supplementation, afforded larger fiber diameters, suggesting that the antioxidants resveratrol and CoQ10 at low dose might afford fiber maturation after regeneration more effectively than in untreated groups. It is furthermore possible that the mechanism that is responsible for hypertrophying of fibers is stimulated by these concentrations of antioxidants.

The variation in fiber diameter in the high CoQ10 and resveratrol/CoQ10 combination groups showed a similar pattern to that of the negative control group. The proportion of fibers with diameters larger than peak values in these groups was larger than in the negative and positive control groups (Figure 5.11). This incidence is not indicative of a hypertrophic incidence as the maximum fiber diameters in the high CoQ10 and resveratrol/CoQ10 groups were found to be only slightly higher than that found in the negative control group (Figure 5.10), although in larger numbers. The observation suggests a more effective maturation of regenerated fibers, and perhaps a reduced occurrence of fiber splitting, consistent with the qualitative histopathology data.

The prevalence of maximum values is also slightly higher in the high CoQ10 and resveratrol/CoQ10 combination groups compared to the negative control group. These values were found to be still smaller than that in the resveratrol and low CoQ10 groups, indicating a lower hypertrophic tendency in the high CoQ10 and resveratrol/CoQ10 combination groups.

5.3.3.2 Hypertrophic Fibers

Paul and Rosenthal, 2002, formulated a definition for hypertrophy, where hypertrophy of skeletal muscle is defined as an increase in the size of fibers without an increase in their number, irrespective of any increase in the number of nuclei per fiber. Consistent with this definition, they have demonstrated that intrafascicularly terminating fibers are elongated in response to hypertrophic stimuli without an increase in fiber number (Paul and Rosenthal, 2002).

Fibers with large diameters (>110µm), although in small numbers, were observed, in addition to the age control group, also in the resveratrol, low CoQ10, high CoQ10 and resveratrol/CoQ10 combination groups. These values are indicative of the presence of a hypertrophic tendency. Hypertrophic skeletal muscle fibers are characterized by a cross-sectional area significantly increased above the normal range established for the age and sex of the individual (Carpenter and Carpati, 1984). Weller and coworkers, 1997, reported hypertrophied fiber in SJL/J mice to measure >100µm. Carpenter and Karpati, 1984, reported that hypertrophic fibres may be quite numerous in Duchenne dystrophy, even in areas where necrosis is not prevalent.

Maximum diameters in DMD may reach well over 100µm, and the mechanism of their production is likely to be analogous to that in experimental compensatory hypertrophy (Carpenter and Karpati, 1984). The primary stimulus to this hypertrophy is believed to be stretch exerted on the sarcomeres, rather than simple over activation of muscle fibers (Hall-Craggs, 1972, in Carpenter and Karpati, 1984). Carpenter and Karpati, 1984, stated that hypertrophic fibers have a tendency to exhibit architectural abnormalities, and that centrally situated nuclei are commonly seen in these fibers. Such fibers have also been found to reveal an increased incidence of apparent longitudinal splitting, and disorientation of myofibrils, like snake coil formations (Carpenter and Karpati, 1984). When a muscle fiber hypertrophies, the maintenance of the normal equilibrium between muscle volume to capillary ratio, requires a proportionate increase of perifiber capillary density (Carpenter and Karpati, 1984). If this adjustment of the capillary bed, required for normal metabolic functioning of the cell mass, is insufficient, it may lead to vulnerability of muscle fibers to ischemic damage (Carpenter and Karpati, 1984). Therefore, the incidence of moth-eaten appearance of fibers may occur especially in hypertrophic fibers due to the increased oxidative enzyme reactions (Carpenter and Karpati, 1984).

5.3.3.3 Variation in Gastrocnemius Muscle Fibers

A definite lower range of maximum diameters compared to that measured in the quadriceps muscle samples was recorded in gastrocnemius muscle samples (Table 5.2). Mean values were lower, while minimum values were higher than that measured in the quadriceps samples (Figure 5.14).

The resveratrol/CoQ10 combination group showed the highest similarity to the negative control group (Figure 5.12), with regard to the minimal, mean and maximum diameters measured. When comparing the distribution of size between these two groups (Figure 5.13), both showed peak values between 60 and 70µm, but the resveratrol/CoQ10 combination group showed an 'accumulation' of fibers (≈62.3% of fibers) sized between 20 and 60µm, while ≈45.8% of fibers were evenly distributed towards the peak size range in the negative control group. Although the variation (Figure 5.12) in the resveratrol/CoQ10 combination group showed high similarity to the unaffected group the size distribution histograms indicated that the fibers were affected by the disease.

Variation in fiber size of the positive control group's gastrocnemius muscles (Table 5.2) was similar to that of the age control group's quadriceps muscle, with the exception of larger maximum values in the age control's quadriceps. This indicates that gastrocnemius fibers show similarity to a younger phenotype, confirming that distal muscles in the SJL/J mice become affected later than the proximal muscles.

The antioxidant supplemented groups displayed a fiber size distribution where all peak values ranged between 50 and 60µm, with the larger proportion of fibers distributed towards smaller fiber size ranges. The resveratrol/CoQ10 combination displayed the same peak levels as the negative control group, with the exception of a larger proportion of fibers towards smaller diameters, following this combination of antioxidant supplementation.

5.3.3.4 From the Morphometeric Results

Collectively, the data suggests that antioxidant supplementation might direct muscle fibers' fate towards a more favorable state, whereas a larger number of fibers in supplemented groups displayed larger diameters than in the untreated groups. This might suggest that high dose antioxidant supplementation, by an undefined mechanism, is able to mediate fiber maturation after regeneration and perhaps the process of regeneration itself. A similar suggestion cannot be made for lower doses of antioxidants. The histopathology data from the resveratrol and low CoQ10 groups does not support the notion of more efficient regeneration or maturation, suggested by the fiber diameter distribution. In turn, fibers from these two groups displayed a hypertrophic tendency.

Collectively, these results suggest that the quadriceps muscles are more affected by the ongoing dystrophic process at the age of 27 weeks than the gastrocnemius muscles. Furthermore, it appears that supplementation with high levels of CoQ10 and resveratrol/CoQ10 in combination, afforded the least variation in quadriceps fiber size in SJL/J mice at 27 weeks of age.

5.4 Concluding Remarks

Bittner and co-workers found that the first histological changes could be observed as early as three weeks of age in the SJL/J mouse model. By seven months, the dystrophic changes include the appearance of fatty and fibrotic tissue, as well as inflammatory foci (Bittner *et al*., 1999). Proximal muscle groups were found to be primarily affected by these changes, whereas the distal muscles remained less affected (Bittner *et al*., 1999). It was therefore decided to analyse the quadriceps muscles of SJL/J mice for the cellular effect of antioxidant supplementation. Quadriceps was expected to represent the most reliable illustration of the condition. While muscle weakness can be detected as early as three weeks of age the greatest pathology occurs after 6 months of age (www.jax.org/jaxmice; Fox, 2007). Between different groups of 6 month old SJL/J mice, Weller and co-workers, 1997, found the percentage of individual animals with active disease to vary from 60% to 100%, averaging 78% of mice overall. It was therefore decided, in order to obtain a histological picture representative of full blown dysferlinopathy, to enter the animals in the present study into a 90-day trial at the age of 14 weeks, in order for them to display the greatest pathology by the termination date.

Histopathological data from the present study has confirmed that distal muscles are less affected and relatively spared in initial phases of the disease in SJL/J mice. The histological picture of the gastrocnemius muscle samples showed little to no dystrophic changes (data not shown), compared to samples from the quadriceps muscles (Figure 5.2 to 5.8). Fiber size variation in gastrocnemius fibers showed a shift towards that of a younger phenotype where all peak values ranged between 50 and 60µm, with the larger proportion of fibers distributed towards smaller fiber size ranges (Figure 5.14). A distinct lower number of nuclei in the central position were observed in gastrocnemius fibers (Figure 5.14).

Evident from the histopathological assessment of quadriceps fibers from 27 week-old SJL/J mice, is a constant influx of inflammatory infiltrate into tissue subjected to dystrophic changes. This finding is supported by the work of Chiu and co-workers, who reported an ongoing inflammatory reaction to be the result of attenuated muscle regeneration in dysferlin-deficient muscle that, together with a membrane repair defect, triggers dystrophic pathology. Consistent with this report, the present

study revealed a shift in fiber size predominance towards smaller fiber sizes in 27 week-old untreated SJL/J mice. The fiber size predominance accounted for a lack of fiber maturation in dysferlin-deficient muscle, resulting in incomplete regeneration in 27 week-old untreated SJL/J mice.

The minimal Feret's diameter parameter offers a useful tool for assessing fiber size variation in the muscle of SJL/J mice. In addition to this measurement, size distribution histograms provided more insight to the exact variation in the fiber size predominance than the mean minimal Feret's diameter alone.

A definite effect of antioxidant supplementation was observed when studying the histograms of quadriceps fiber size distribution (Figure 5.14). The findings provide evidence for the facilitation of fiber maturation in all antioxidant supplemented groups. Histopathological data showed that groups treated with the highest antioxidant concentrations (high CoQ10 and resveratrol/CoQ10 combination) displayed fewer split fibers, a factor influencing the fiber size variation. The fiber size distribution histograms for these two groups suggest that active regeneration occurred in these groups, followed by maturation of fibers towards larger fiber diameters.

In contrast to the untreated positive control group, muscle fibers of SJL/J mice supplemented with lower antioxidant concentrations tend to attain larger fiber sizes, with a tendency towards hypertrophy.

The number of nuclei found in the central position of muscle fibers, displayed a shift towards a lower percentage following supplementation with higher doses of antioxidants. This finding is supportive of an important role of central nuclei as a parameter for dystrophic progression in tissue analysis. Although it is yet to be discovered by what mechanism nuclei exchange their peripheral position for this central location in fibers of dystrophic muscle, it is nevertheless clear that high dose antioxidant supplementation, play a substantial role in altering this process.

Assessment of the histopathology showed, from a qualitative perspective, markedly reduced inflammatory insult in the more affected quadriceps muscles of animals treated with high doses of CoQ10 and a combination of resveratrol/CoQ10. An ongoing inflammatory reaction as the result of attenuated muscle regeneration in dysferlin-deficient muscle (Chiu *et al*., 2009), was markedly reduced. When taking the work of Chiu's team into account, collectively the findings of the present chapter allude to the ability of high doses of CoQ10 and resveratrol/CoQ10 in combination, to decrease the ongoing inflammatory process. The morphometeric analyses from these two groups

provide evidence strengthening the suggestion that a reduction in inflammatory processes resulted in more efficient muscle regeneration, followed by fiber maturation.